

PHAROS

THE GREEK AI FACTORY

AI4Health Track

Training Series

Course 5

Trustworthy and Explainable AI in Health

MARCH 13, 2026 | 12:00 EET | ONLINE



EuroHPC
Joint Undertaking



Co-funded by
the European Union

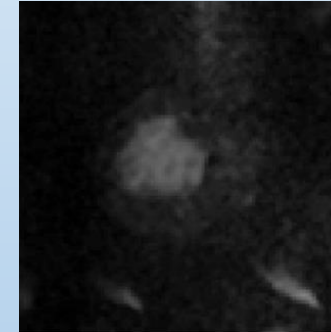
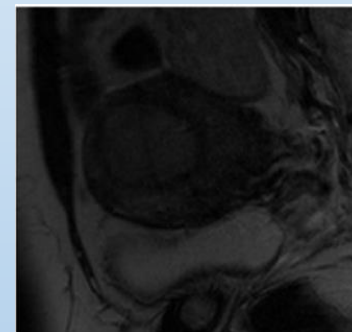
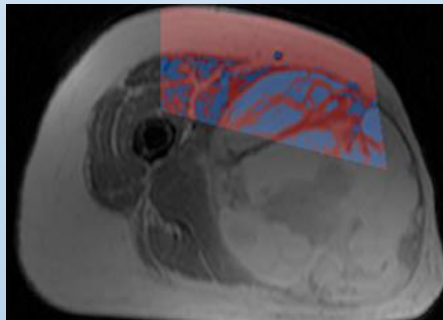
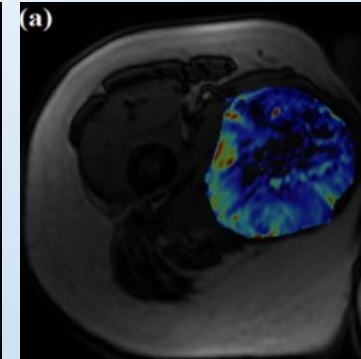
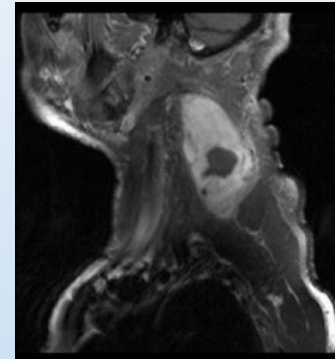
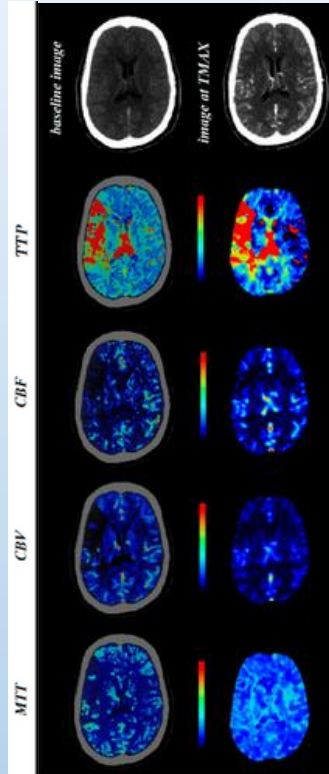
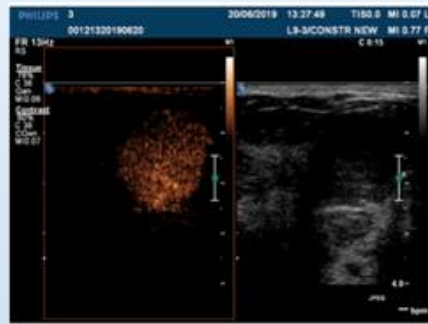
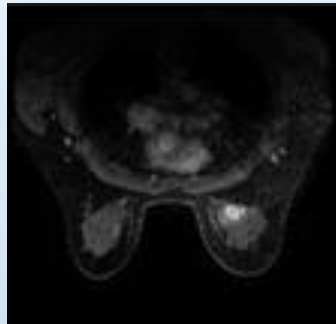


PHAROS
GREECE



ΕΛΛΗΝΙΚΗ ΔΗΜΟΚΡΑΤΙΑ
Υπουργείο Ψηφιακής Διακυβέρνησης
και Τεχνητής Νοημοσύνης

From Quantitative MRI to Explainable AI models: Applications in Cancer Imaging



Post Doctoral Researcher: Computational BioMedicine Laboratory (CBML), Institute of Computer Science, Foundation For Research and Technology-Hellas (FORTH)

Assistant Professor: Radiology – AI in Medicine, 1st Department of Radiology, School of Medicine, Aretaieion Hospital, National and Kapodistrian University of Athens



INSTITUTE OF COMPUTER SCIENCE

<https://www.ics.forth.gr/cbml>



National and Kapodistrian University of Athens

<https://www.radiology1uoa.gr>

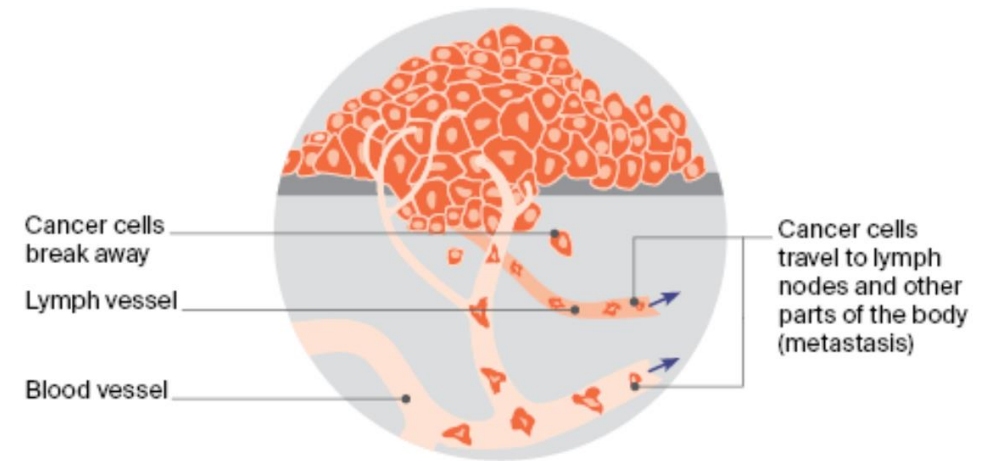
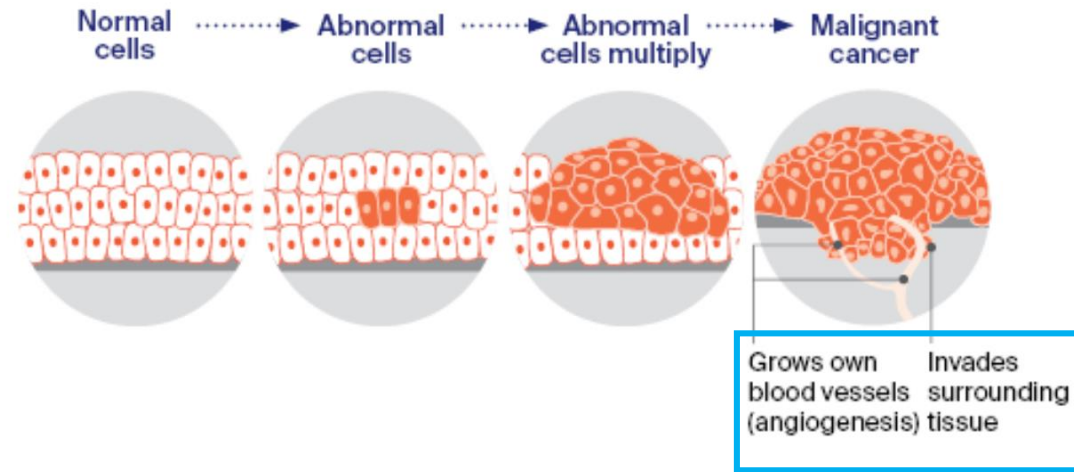
Contents

- Cancer Basics
- Cancer Imaging
 - MRI-perfusion (DCE/DSC)
 - MRI-diffusion (DWI)
- MRI quantification
 - Biomarkers/ Parametric maps
 - Radiomics
- Machine learning with Radiomics
- Explainability in ML
 - Applications
- Conclusion/Discussion

What is Cancer?

Cancer is a large group of diseases characterized by the uncontrolled growth and spread of abnormal cells, which can invade nearby tissues and metastasize to other parts of the body.

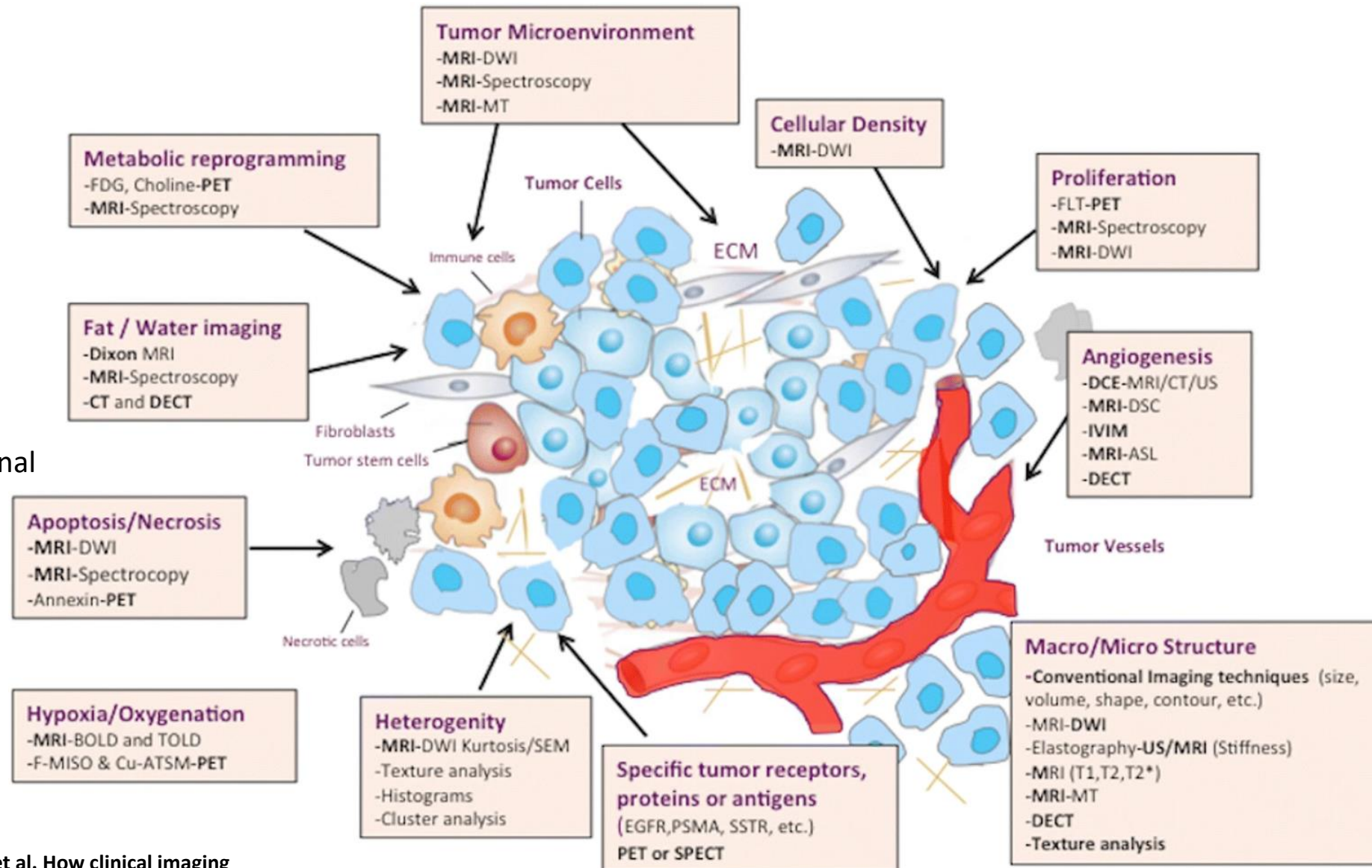
Unlike normal cells, cancer cells ignore signals to stop dividing or die, often forming tumors.



How clinical imaging can assess cancer biology

Modality of choice:

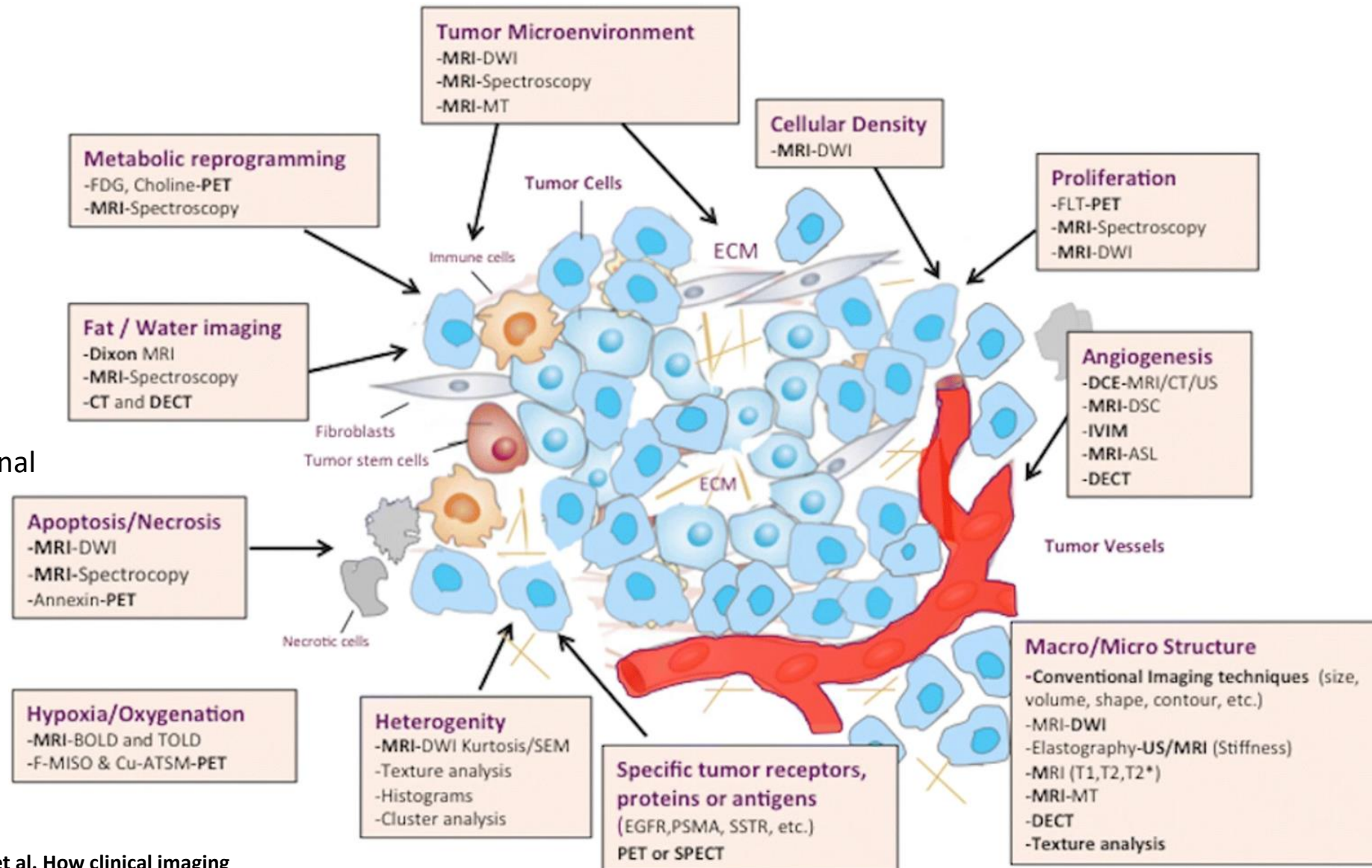
- Computed Tomography (CT)
 - Detailed Anatomy
- X-Rays
 - 2D projectional images
- Ultra Sound
 - Fast, Cheap, Easily accessible
 - Low resolution/One dimensional
- PET
 - Metabolic Activity
 - Low spatial resolution
- MRI
 - High resolution
 - Anatomical Images
 - Functionality
 - Non conventional Imaging



How clinical imaging can assess cancer biology

Modality of choice:

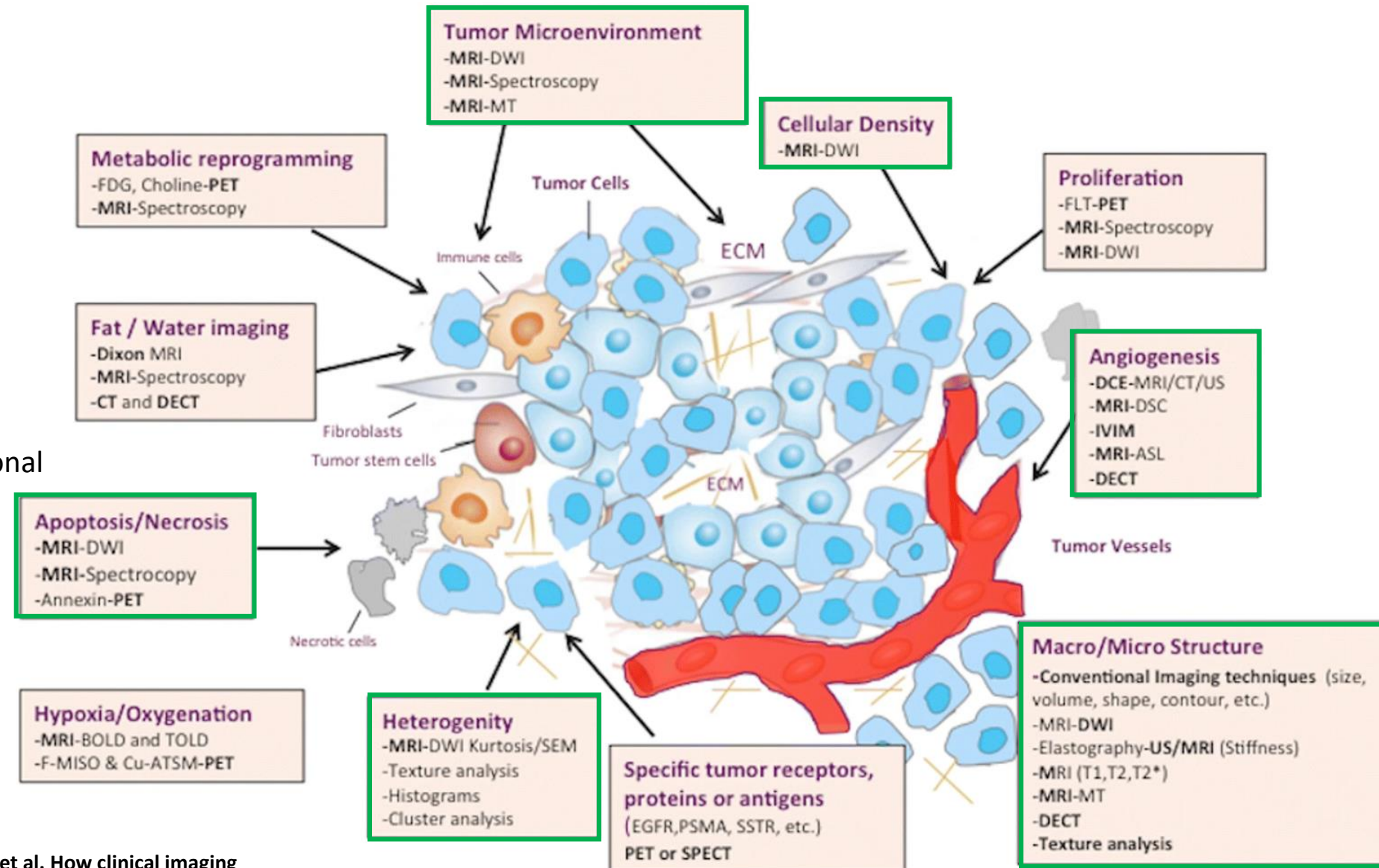
- Computed Tomography (CT)
 - Detailed Anatomy
- X-Rays
 - 2D projectional images
- Ultra Sound
 - Fast, Cheap, Easily accessible
 - Low resolution/One dimensional
- PET
 - Metabolic Activity
 - Low spatial resolution
- **MRI**
 - High resolution
 - Anatomical Images
 - Functionality
 - Non conventional Imaging



How clinical imaging can assess cancer biology

Modality of choice:

- Computed Tomography (CT)
 - Detailed Anatomy
- X-Rays
 - 2D projectional images
- Ultra Sound
 - Fast, Cheap, Easily accessible
 - Low resolution/One dimensional
- PET
 - Metabolic Activity
 - Low spatial resolution
- MRI
 - High resolution
 - Anatomical Images
 - Functionality
 - Non conventional Imaging



Magnetic Resonance Imaging (MRI)

MRI - Relaxation

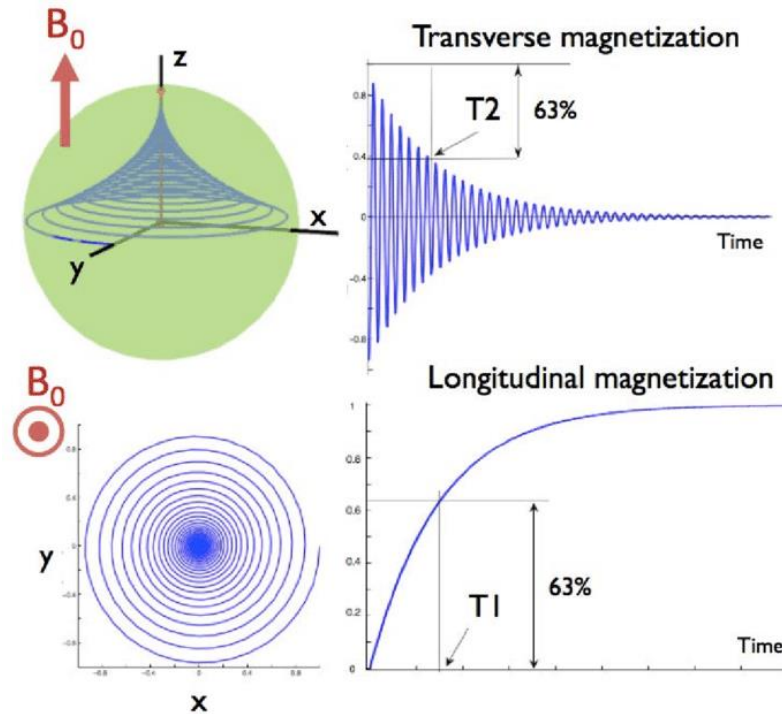
MRI

Perfusion Imaging

Dynamic Contrast Enhanced (DCE)
Dynamic susceptibility contrast (DSC)

Diffusion Weighted Imaging

Apparent Diffusion Coefficient (ADC)
IVIM



T2 relaxation time is defined as the time needed to dephase up to 37% of the original value.

T1 (longitudinal relaxation time) is defined as the time needed to achieve 63% of the original longitudinal magnetization (in Z axis).

Each tissue has its own T1/T2 relaxation time and curve.

- Concurrently happening, T1-w or T2-w
- T1 constant > T2 constant

Magnetic Resonance Imaging (MRI)

MRI

Perfusion Imaging

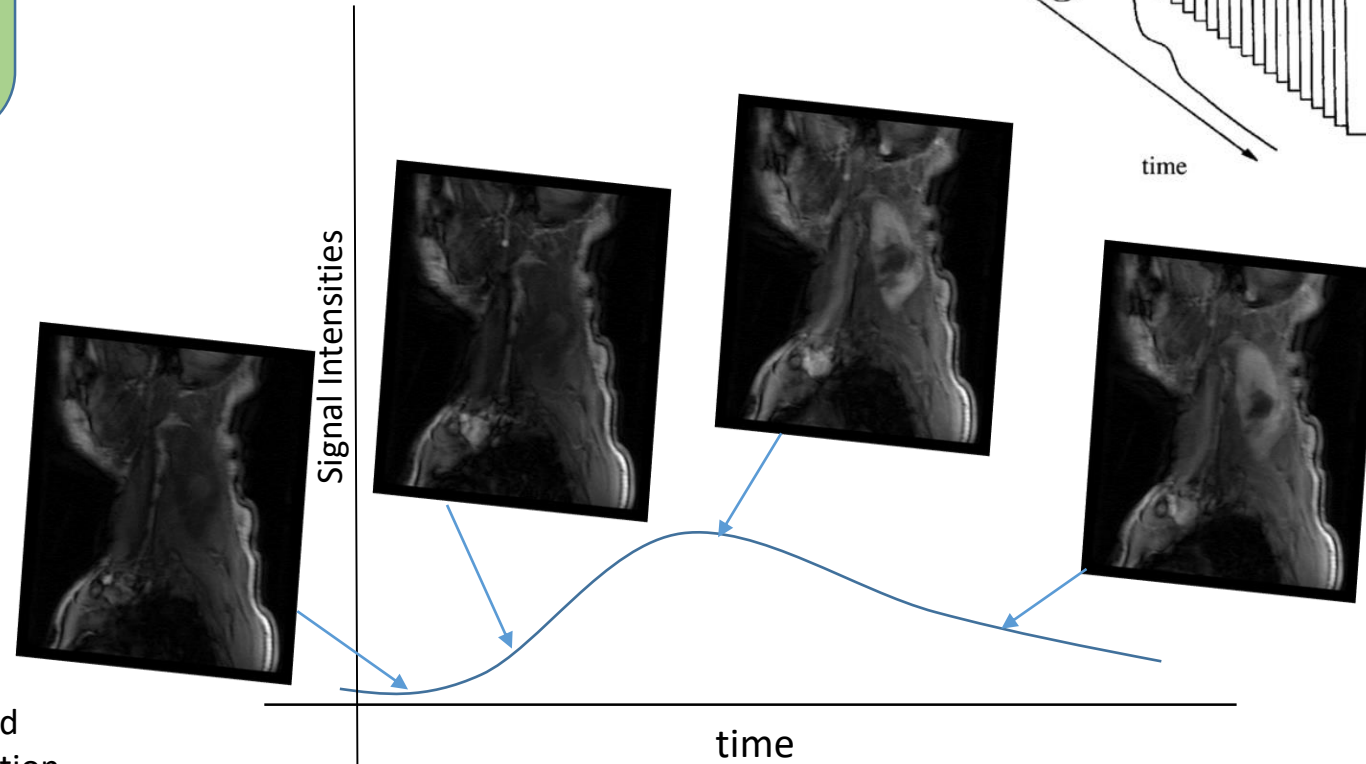
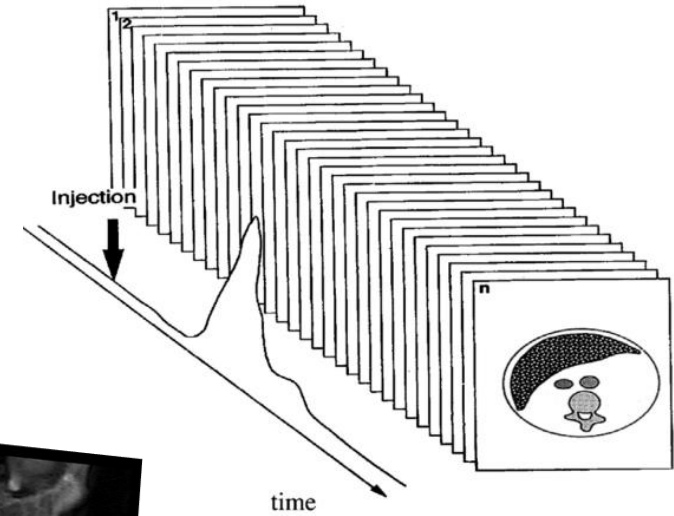
Dynamic Contrast Enhanced (DCE) T1w

Dynamic susceptibility contrast (DSC) T2w

Diffusion Weighted Imaging

Apparent Diffusion Coefficient (ADC)

IVIM



Sequential acquisition dynamic contrast enhanced Imaging is performed before and during the injection of contrast agent.

Perfusion Curves

DCE-MRI Quantification – Parametric maps

MRI

Perfusion Imaging

Dynamic Contrast Enhanced (DCE) T1w

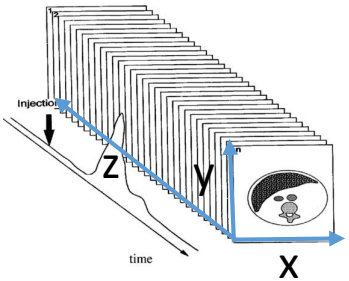
Dynamic susceptibility contrast (DSC) T2w

Diffusion Weighted Imaging

Apparent Diffusion Coefficient (ADC)

IVIM

4D data $[x,y,z,t]$



Given

ROI-Region of interest

Model/target Function $M(\mathbf{x},t)$

Fit $M(\mathbf{x},t)$ to the data/ Perfusion Curve:

On a voxel basis

Obtain: x_1, x_2, x_3, x_4

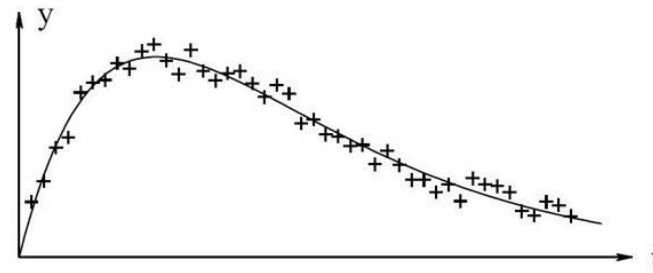
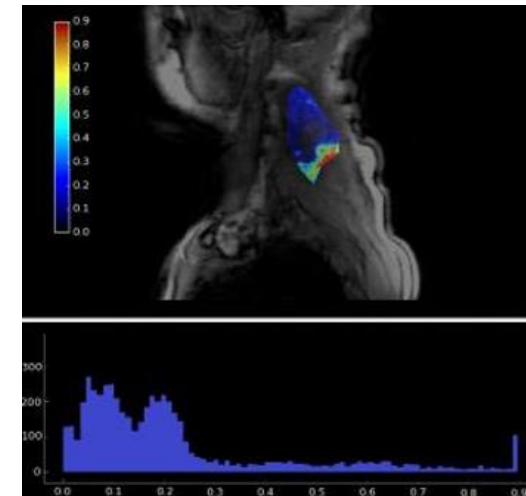
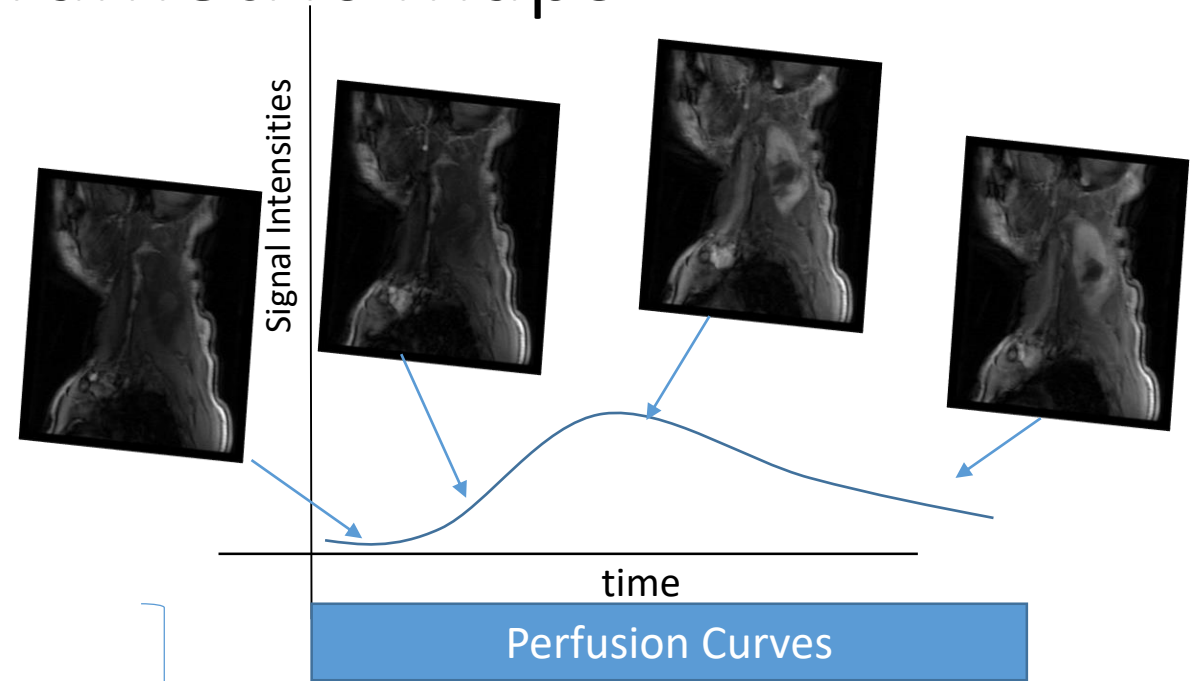


Figure 1.1. Data points $\{(t_i, y_i)\}$ (marked by +) and model $M(\mathbf{x}, t)$ (marked by full line.)

$$M(\mathbf{x}, t) = x_3 e^{x_1 t} + x_4 e^{x_2 t}$$



DCE-MRI Quantification – Parametric maps

MRI

Perfusion Imaging

Dynamic Contrast Enhanced (DCE) T1w

Dynamic susceptibility contrast (DSC) T2w

Diffusion Weighted Imaging

Apparent Diffusion Coefficient (ADC)

IVIM

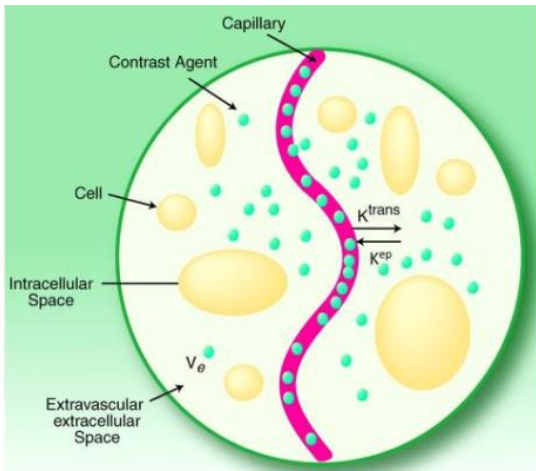


Figure: Compartmental modeling

- $C_t(t)$ • Contrast agent's concentration at tissue
- K_{trans} • Transfer constant from blood plasma to EES
- $C_a(t)$ • Contrast agent's concentration at a feeding artery
- K_{ep} • Transfer constant from EES to blood plasma
- v_p • Blood plasma volume

[28] Extended Tofts Model: $C_t(t) = K_{trans}e^{-K_{ep}t} \otimes C_a(t) + v_p C_a(t)$

[29] Patlak Model: $C_t(t) = K_{trans} \int_0^t C_a(\tau) d\tau + v_p C_a(t)$

[30] Buckley Model: $C_t(t) = v_p C_a(t)$

[31] GCTT Model:

$$C_t(t) = F \left[\gamma \left(\frac{1}{a^{-1}}, \frac{t}{\tau} \right) + \frac{E e^{-K_{ep}t}}{(1 - K_{ep}\tau)^{1/a^{-1}}} \left[1 - \gamma \left(\frac{1}{a^{-1}}, \left(\frac{1}{\tau} - K_{ep} \right) t \right) \right] \right] \otimes C_a(t)$$

[33] Tofts Model: $C_t(t) = K_{trans}e^{-K_{ep}t} \otimes C_a(t)$

[28] P. S. Tofts, G. Brix, D. L. Buckley, J. L. Evelhoch, E. Henderson, M. V. Knopp, H. B. Larsson, T. Y. Lee, N. A. Mayr, G. J. Parker, R. E. Port, J. Taylor, and R. M. Weisskoff, "Estimating kinetic parameters from dynamic contrast-enhanced T(1)-weighted MRI of a diffusible tracer: standardized quantities and symbols.," *Journal of magnetic resonance imaging : JMRI*, vol. 10, pp. 223–32, sep 1999.

[29] C. S. Patlak, R. G. Blasberg, and J. D. Fenstermacher, "Graphical Evaluation of Blood-to-Brain Transfer Constants from Multiple-Time Uptake Data," *Journal of Cerebral Blood Flow & Metabolism*, vol. 3, pp. 1–7, mar 1983.

[30] S. P. Sourbron and D. L. Buckley, "Classic models for dynamic contrast-enhanced MRI," *NMR in Biomedicine*, vol. 26, no. 8, pp. 1004–1027, 2013.

[31] M. C. Schabel, "A unified impulse response model for DCE-MRI.," *Magnetic resonance in medicine*, vol. 68, pp. 1632–46, nov 2012.

[33] P. S. Tofts, "Modeling tracer kinetics in dynamic Gd-DTPA MR imaging.," *Journal of magnetic resonance imaging : JMRI*, vol. 7, no. 1, pp. 91–101, 1997.

Magnetic Resonance Imaging (MRI)

MRI

Perfusion Imaging

Dynamic Contrast Enhanced (DCE) T1w

Dynamic susceptibility contrast (DSC) T2w

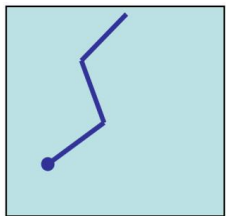
Diffusion Weighted Imaging

Apparent Diffusion Coefficient (ADC)

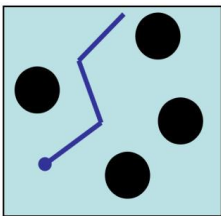
IVIM

- Diffusion Weighted Imaging (DWI) is an important noninvasive method for the diagnosis and follow up of oncologic patients.
- Water molecules motion provides information about the cellularity degree of the tissues.
- The amplitude and duration of the diffusion gradients is represented by the “b-value” (in s/mm^2), an index used to control the sensitivity of DWI contrast to water mobility

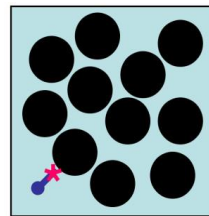
- Diffusion is a random walk (Brownian motion)
- Characterized by the Diffusion constant D



Random
Brownian Motion



Free diffusion
Low signal intensity DWI
High ADC



Restricted diffusion
High signal intensity DWI
Low ADC

• water molecule



cell

Diffusion Signal Decay:
$$\frac{S_b}{S_0} = e^{-bD}$$

- b , b-value in (s/mm^2) (parameter that affects diffusion sensitivity)
- $S(b)$, the signal
- S_0 , the signal without diffusion sensitivity
- No contrast agent required

DW-MRI Quantification

MRI

Perfusion Imaging

Dynamic Contrast Enhanced (DCE)
Dynamic susceptibility contrast (DSC)

Diffusion Weighted Imaging

Apparent Diffusion Coefficient (ADC)
IVIM

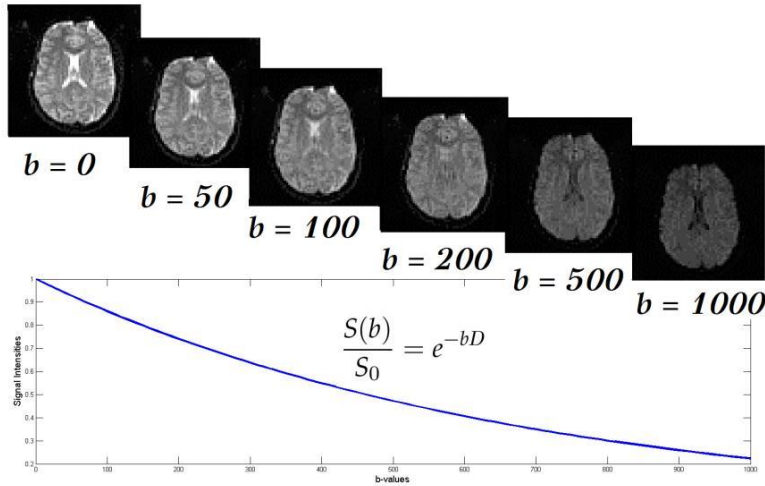
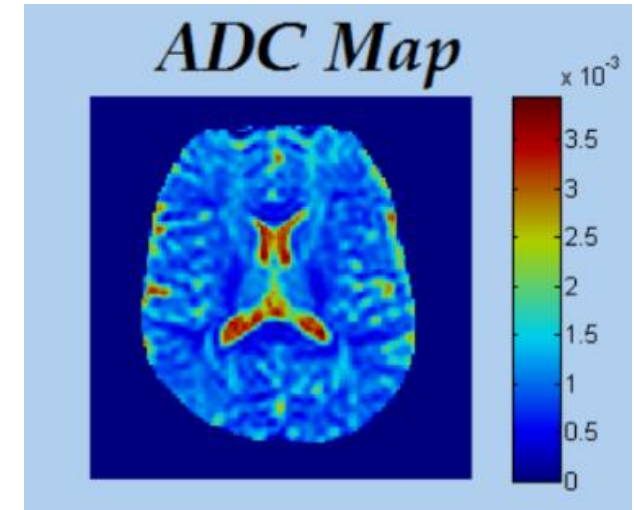


Figure: Signal as function of the b-value

Similarly to Perfusion

Fit $M(\mathbf{x}, t)$ to the data/ Diffusion Curves
On a voxel basis
Obtain: D/ADC



- $ADC = \frac{1}{(b_j - b_i)} \ln \left[\frac{S(b_i)}{S(b_j)} \right]$
- Linear least squares to: $\log(S(b))$
- Non-Linear least squares to:
 $S(b) = S_0 e^{-bD}$

Diffusion Curves

DW MRI – IVIM modeling

MRI

Perfusion Imaging

Dynamic Contrast Enhanced (DCE)
Dynamic susceptibility contrast (DSC)

Diffusion Weighted Imaging

Apparent Diffusion Coefficient (ADC)
IVIM

IVIM-model

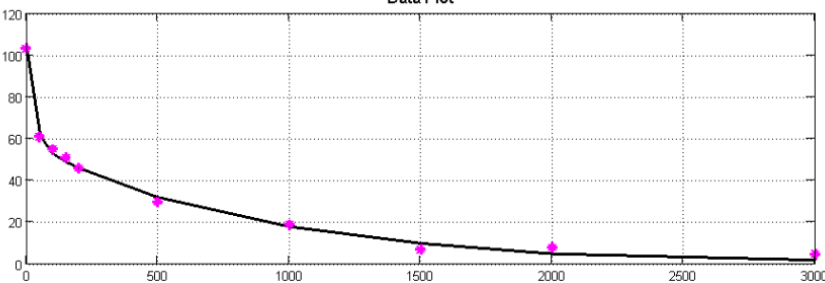
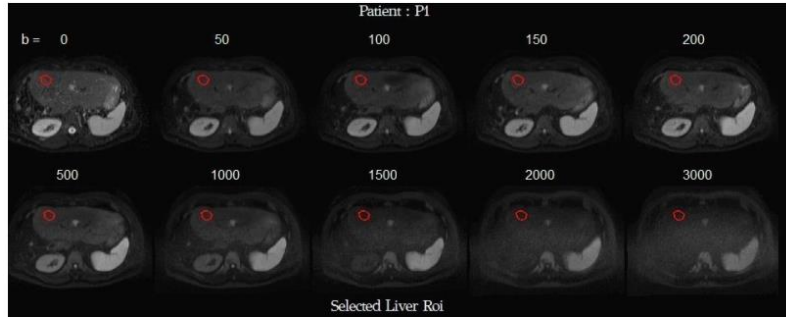
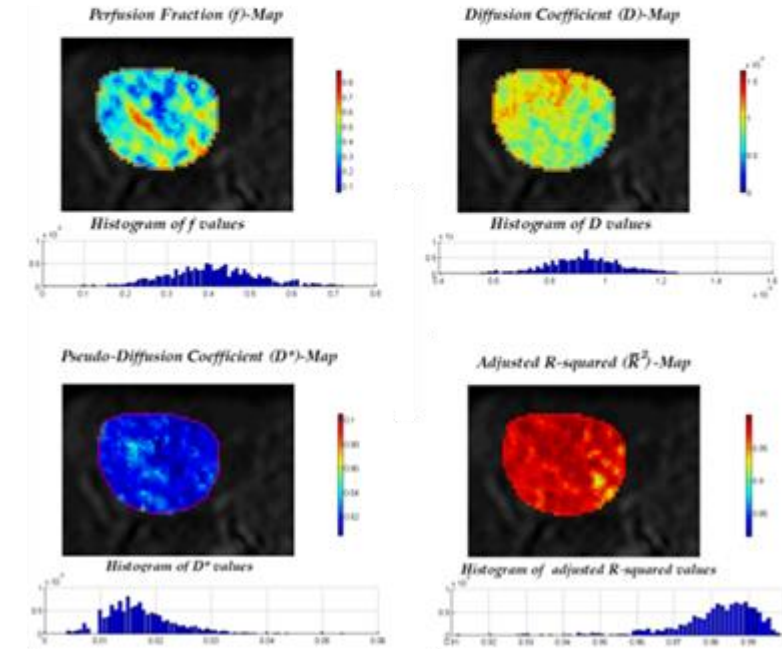
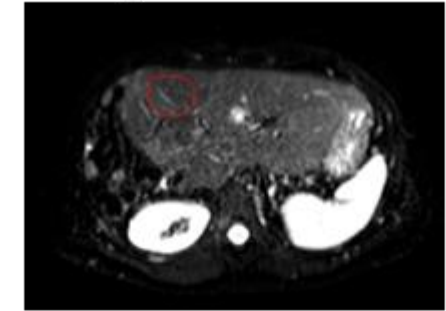
Intra-Voxel Incoherent motions
Blood perfusion (capillary network)
also contributes to signal decay

$$\frac{S_b}{S_0} = (1 - f)e^{-bD} + fe^{-bD^*}$$

Fit IVIM function to the data
On a voxel basis
Obtain: f, D, D^*

f micro-perfusion fraction, $f \in [0, 1]$

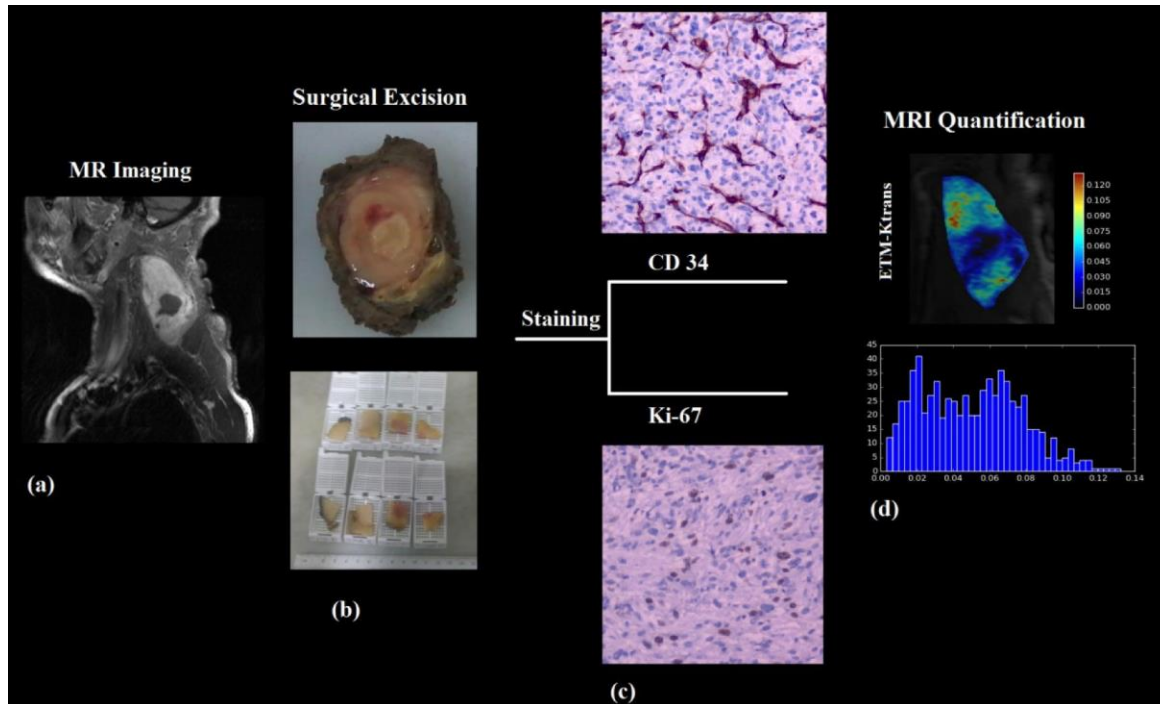
- D Diffusion Coefficient
- D^* pseudo-Diffusion coefficient



Diffusion Curves

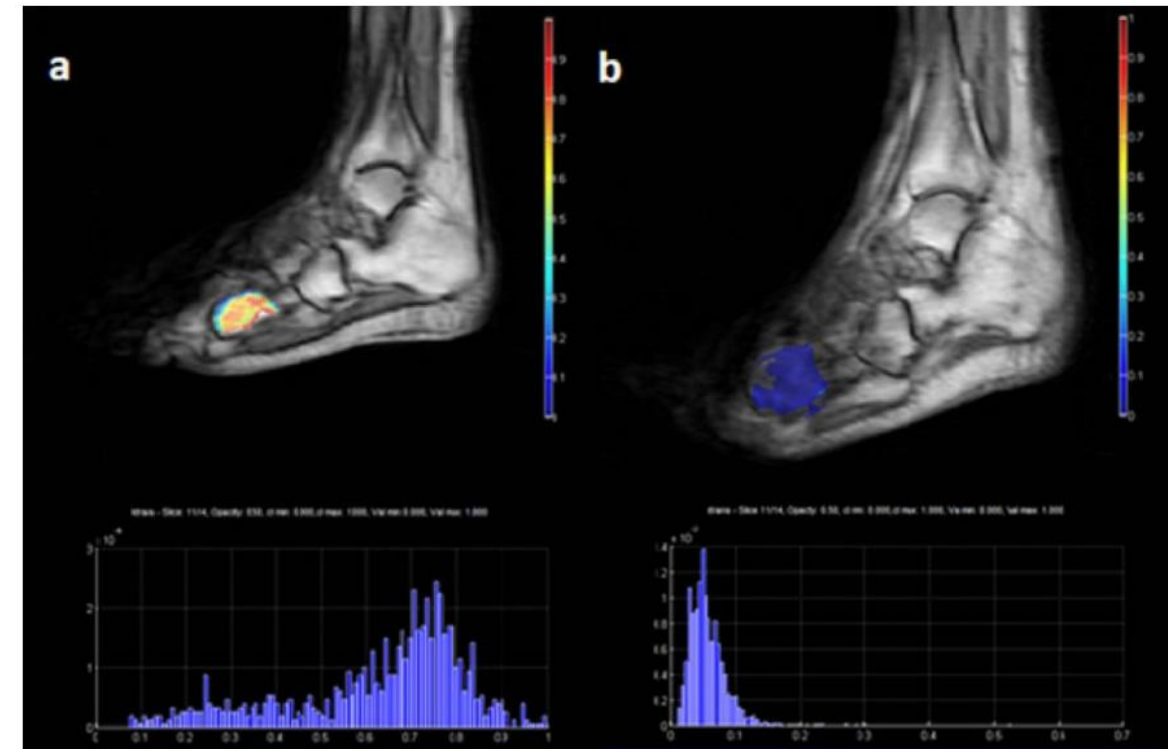
Biomarker Examples (Ktrans)

- Blood perfusion related biomarkers in musculoskeletal cancers



(a) MR imaging (fat suppressed contrast enhanced T1W) of a soft tissue mass in the neck. (b) Surgically excised specimen and tissue preparation sampling for staining. (c) Assessment of vascularity (CD 34) and mitotic activity (Ki-67) based on specific staining. (d) Quantitative analysis of MR data, indicative Ktrans parametric map and the corresponding histogram.

Statistical and spatial correlation between diffusion and perfusion MR imaging parameters: A study on soft tissue sarcomas



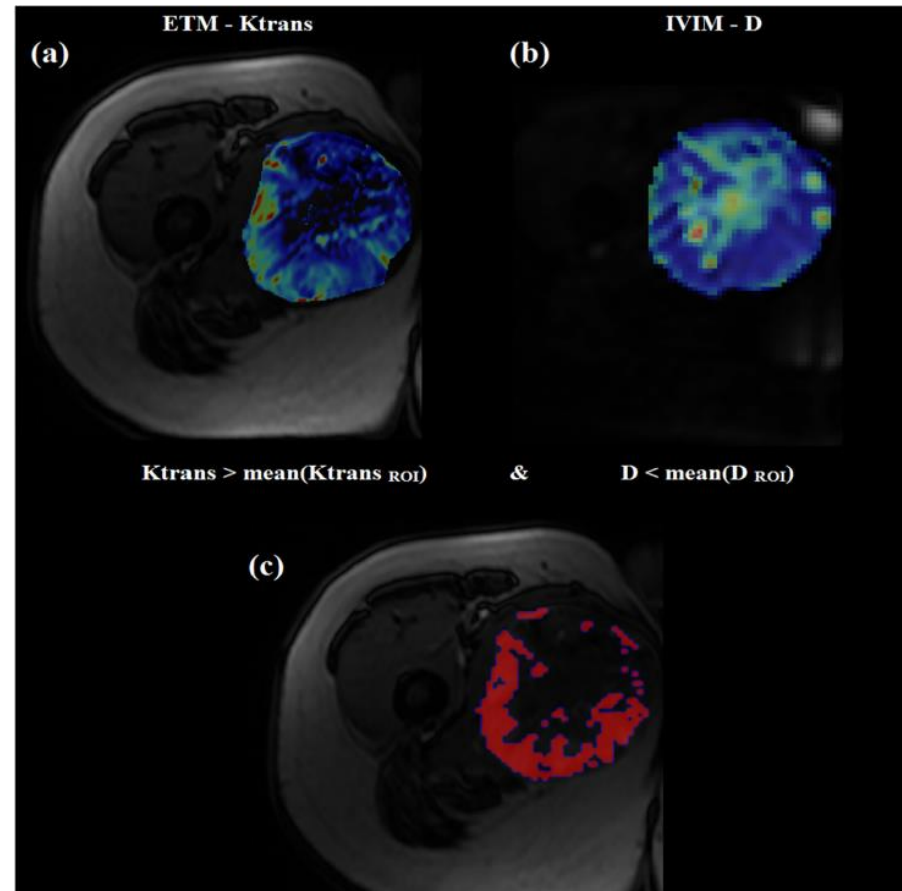
Lower limb sarcoma patient

Ktrans maps a) before, b) after treatment

Perfusion and Oxygenation Changes after Isolated Limb Perfusion with TNF - alpha in Lower Limb Sarcoma: A Case Report

Diffusion – Perfusion Combination

- Aggressive regions of a tumor
- For example:
 - High Ktrans
 - Low ADC



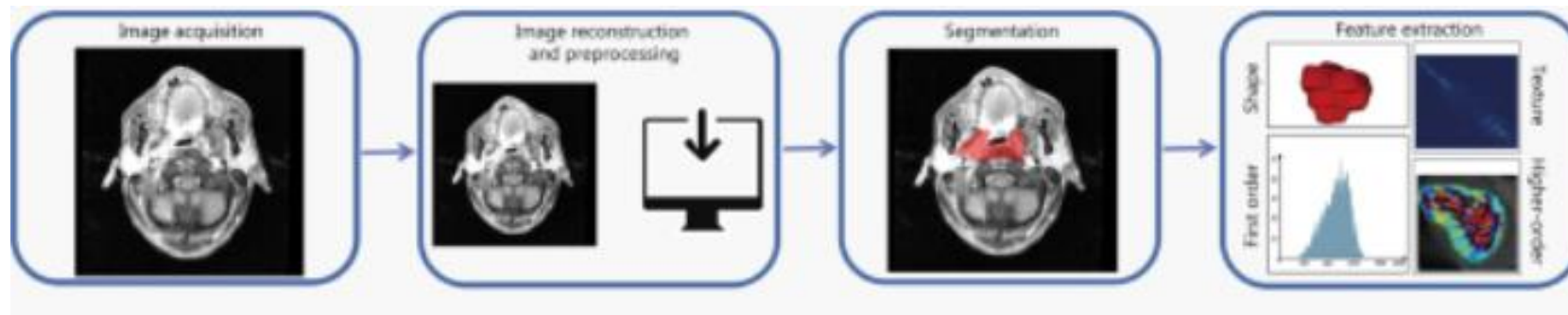
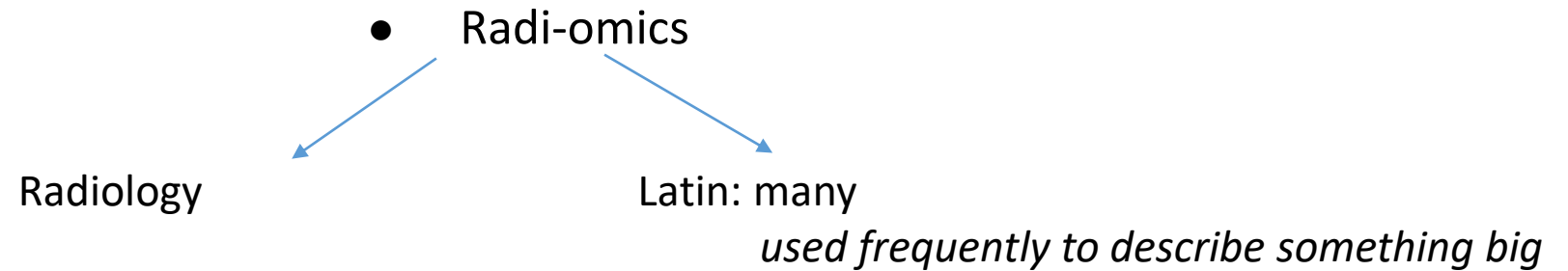
Statistical and spatial correlation between diffusion and perfusion MR imaging parameters: A study on soft tissue sarcomas

Diffusion – Perfusion Combination Prostate Cancer Aggressiveness



Malignancy: High b-values > 800 s/mm² signal and low ADC values

From quantitative information to Radiomics



Radiomic analysis is the process of extracting quantitative features from medical images using complex mathematical algorithms. Its goal is to convert images into data that can be analyzed computationally.

From quantitative information to Radiomics

1. First-Order Features (Intensity-Based Statistics)

- Mean intensity
- Median
- Minimum / Maximum intensity
- Standard deviation
- Variance
- Skewness
- Kurtosis
- Entropy
- Energy
- Uniformity
- Percentiles (e.g., 10th, 90th percentile)

3. Texture Features – GLCM (Gray Level Co-occurrence Matrix)

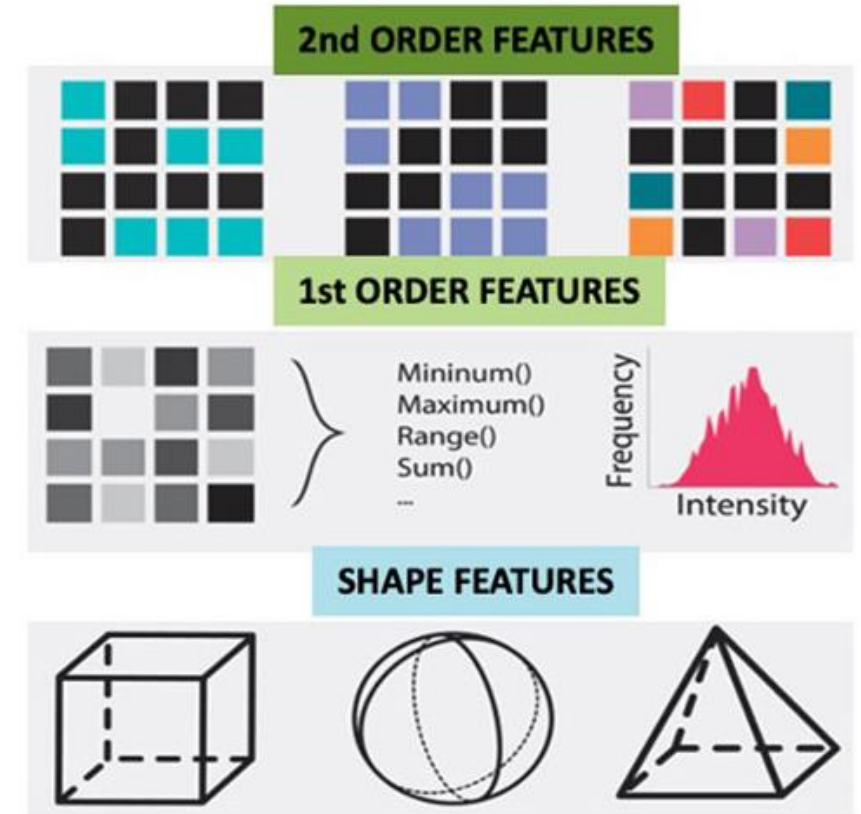
- Contrast
- Correlation
- Homogeneity
- Energy (Angular Second Moment)
- Dissimilarity
- Entropy

3b. Texture Features – GLRLM (Gray Level Run Length Matrix)

- Short Run Emphasis (SRE)
- Long Run Emphasis (LRE)
- Gray Level Non-Uniformity (GLN)
- Run Length Non-Uniformity (RLN)
- Run Percentage

2. Shape-Based Features

- Volume
- Surface area
- Surface-to-volume ratio
- Sphericity
- Compactness
- Elongation
- Flatness
- Maximum diameter
- Bounding box dimensions



RADIOMICS EXTRACTIONS



PyRadiomics

<https://pyradiomics.readthedocs.io>

From quantitative information to Radiomics

3c. Texture Features – GLSZM (Gray Level Size Zone Matrix)

- Small Area Emphasis
- Large Area Emphasis
- Zone Size Non-Uniformity
- Zone Percentage

3d. Texture Features – NGTDM (Neighborhood Gray Tone Difference Matrix)

- Coarseness
- Contrast
- Busyness
- Complexity
- Strength

3e. Texture Features – GLDM (Gray Level Dependence Matrix)

- Dependence Non-Uniformity
- Large Dependence Emphasis
- Gray Level Variance

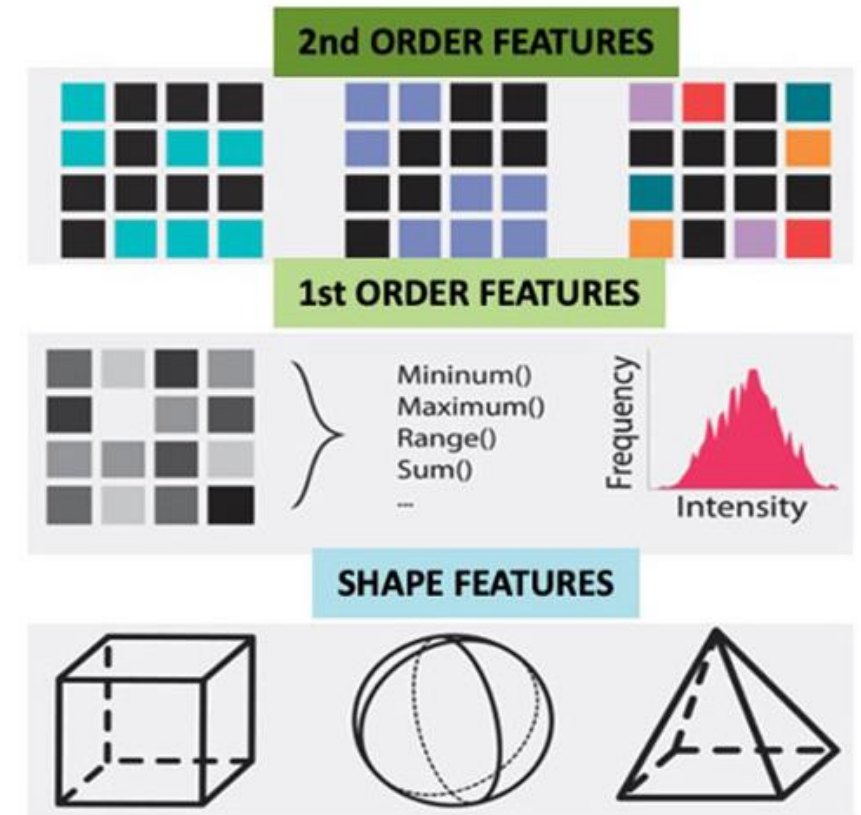
4. Higher-Order (Filtered) Features

- Wavelet features
- Laplacian of Gaussian (LoG) features
- Gradient-based features
- Local Binary Patterns (LBP)
- Fractal features



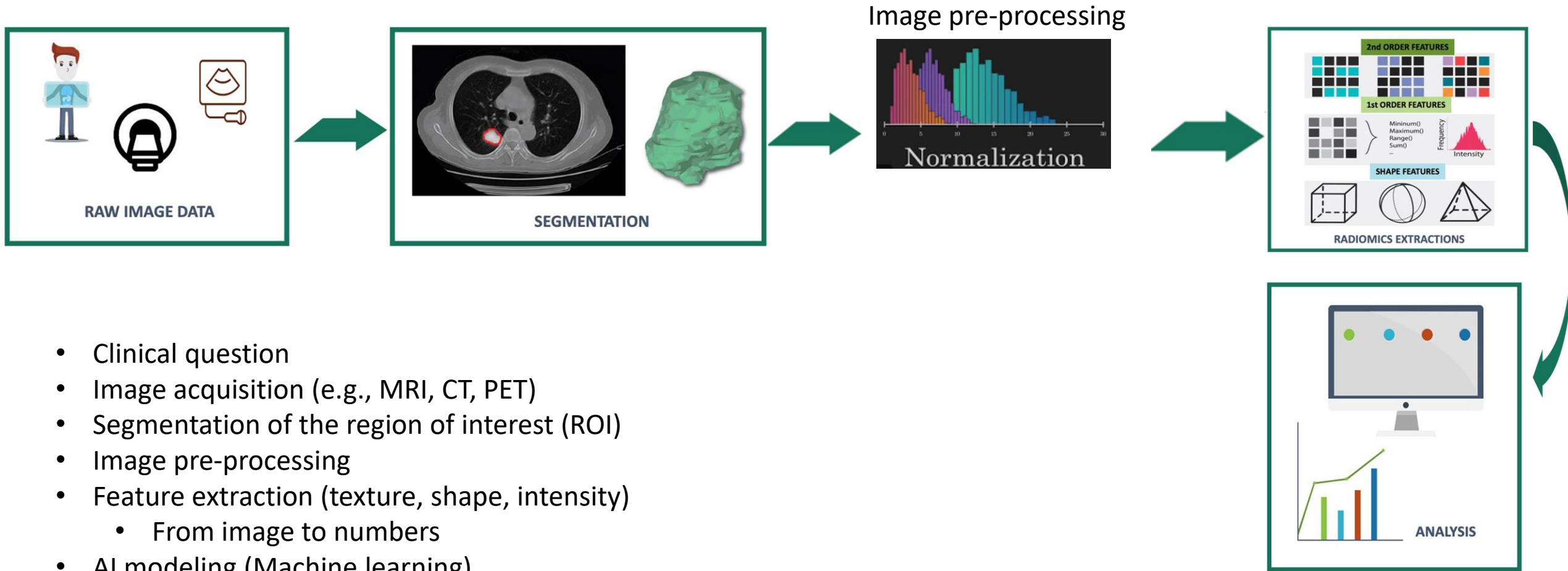
PyRadiomics

<https://pyradiomics.readthedocs.io>



RADIOMICS EXTRACTIONS

Radiomics Workflow

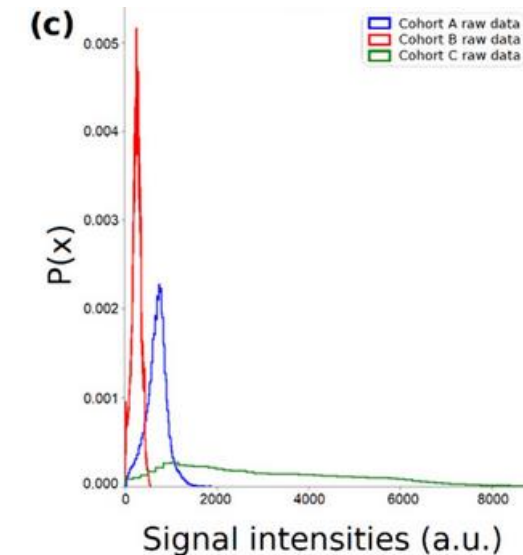
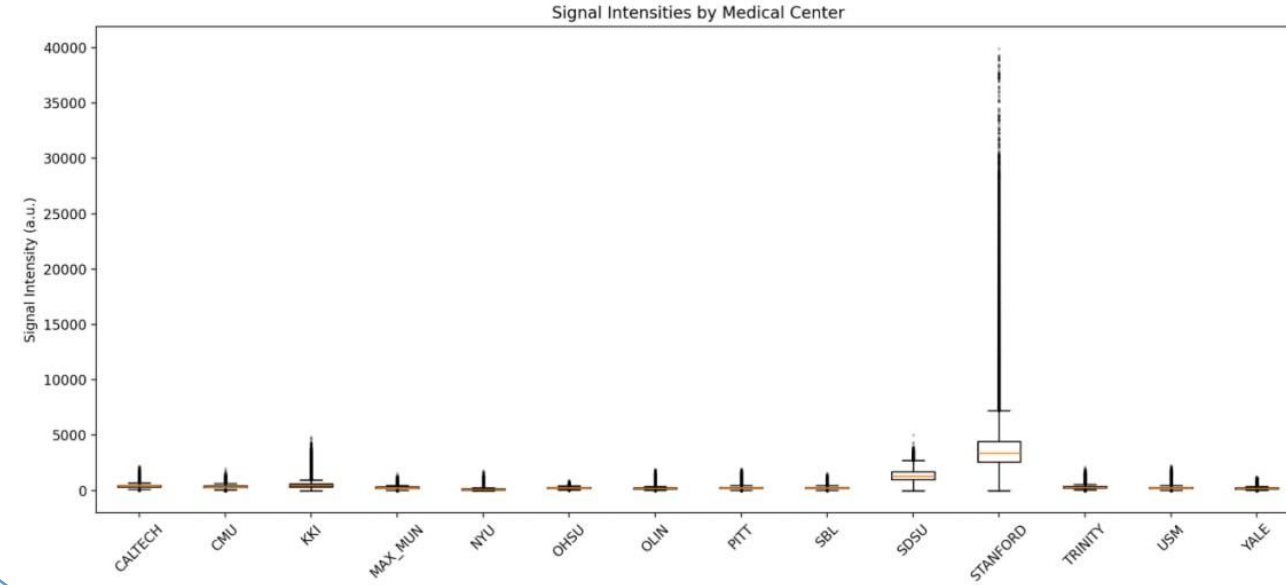


- Clinical question
- Image acquisition (e.g., MRI, CT, PET)
- Segmentation of the region of interest (ROI)
- Image pre-processing
- Feature extraction (texture, shape, intensity)
 - From image to numbers
- AI modeling (Machine learning)
- Interpretation & clinical decision-making

Machine Learning Workflow

- Radiomics Model

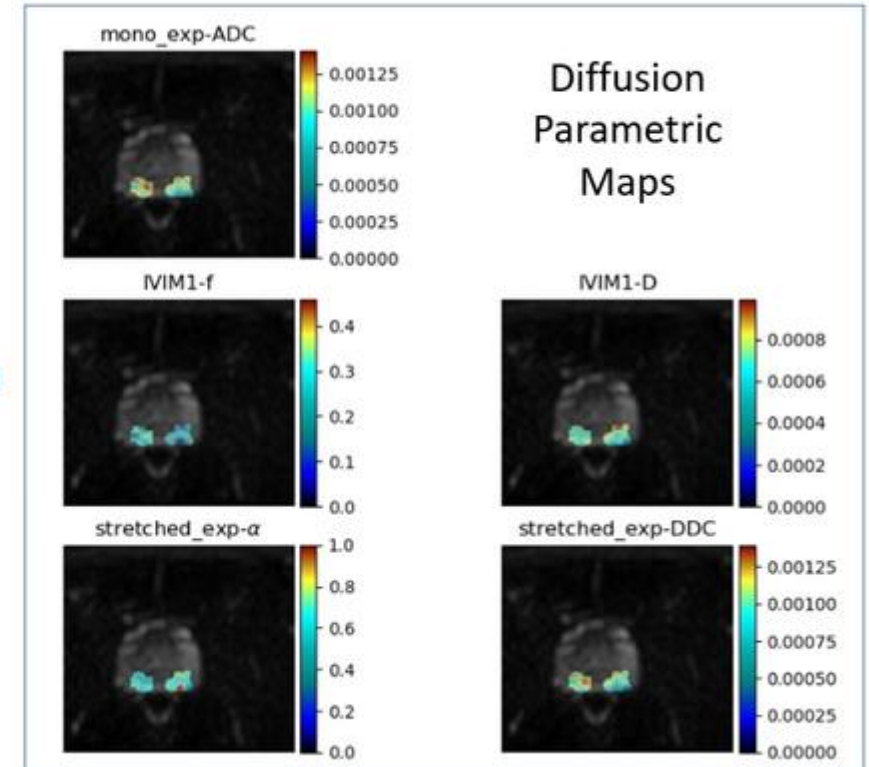
- Clinical question (classification/segmentation)
- Data ()
 - Number of classes
 - Class Imbalance (SMOTE etc.)
 - Data harmonization/normalization
- Radiomic Features extraction
 - First/higher order statistics
 - GLRLM, GLCM, GLSZM, GLDM
 - shape-based 2D and 3D features
 - Logarithmic, Exponential, wavelet transforms
- Feature Selection
 - Lasso, Recursive Feature Elimination
 - ANOVA
- Cross validation scheme
 - K-fold
 - Internal/external validation set
 - Leave one center out cross validation (LOCO)
- Classifiers
 - LogisticRegression, KNeighborsClassifier,
 - RandomForestClassifier, AdaBoost Classifier,
 - GaussianNB
- Performance Evaluation
 - Sensitivity
 - Specificity
 - Accuracy (ACC)
 - AUC
- Explainability
 - SHAP (SHapley Additive exPlanations)
 - Lime (Local Interpretable Model-agnostic Explanations)



Prostate Cancer Aggressiveness Prediction

Clinical Question

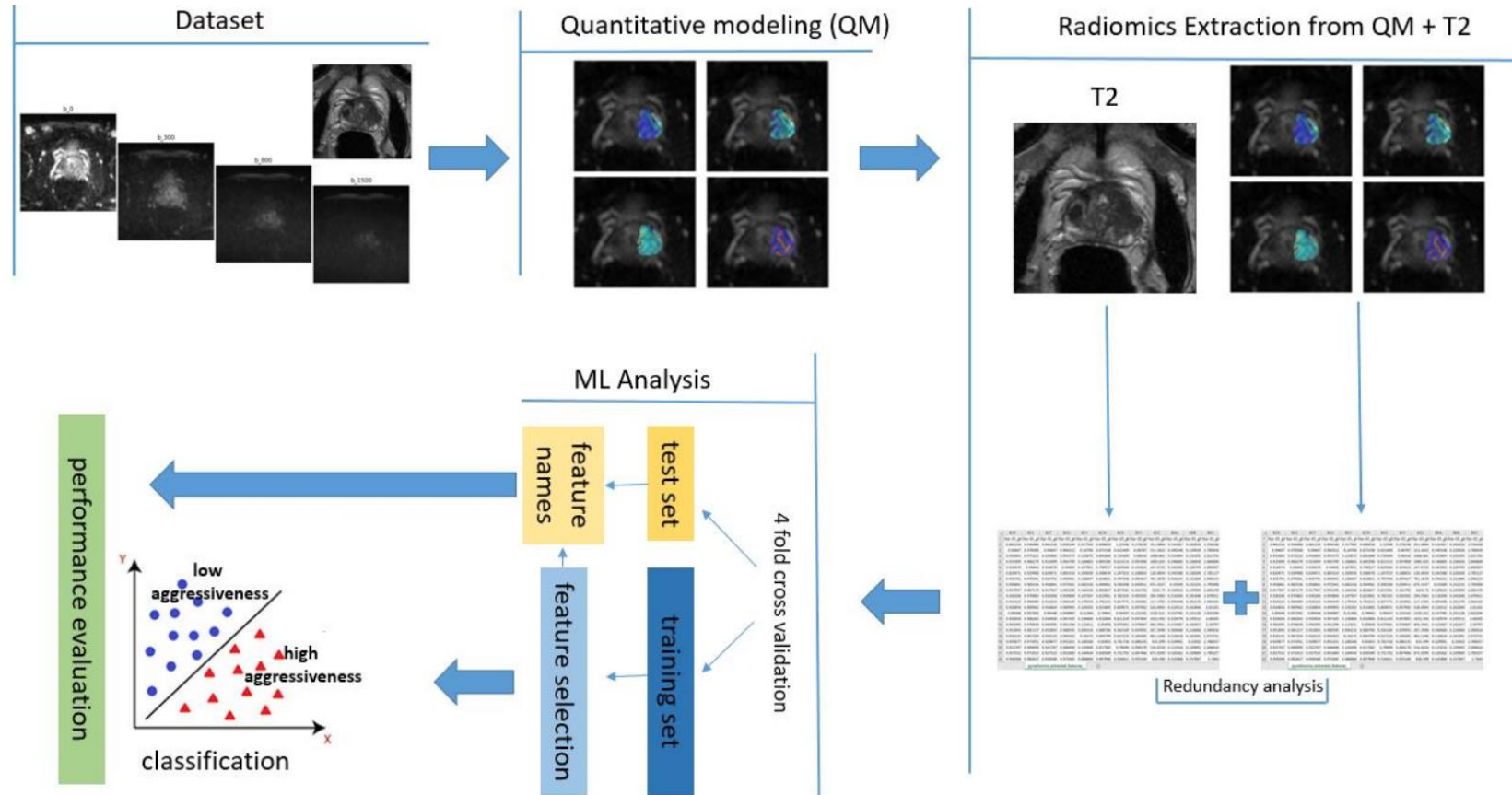
- Classification Problem
 - Aggressive vs. Non Aggressive Cancer
-
- Data T2w images
 - Multi b-value DWI images
 - Diffusion Parametric maps
-
- T2 Radiomics
 - Parametric Map Radiomics



Prostate Cancer Aggressiveness Prediction

- Radiomics Model

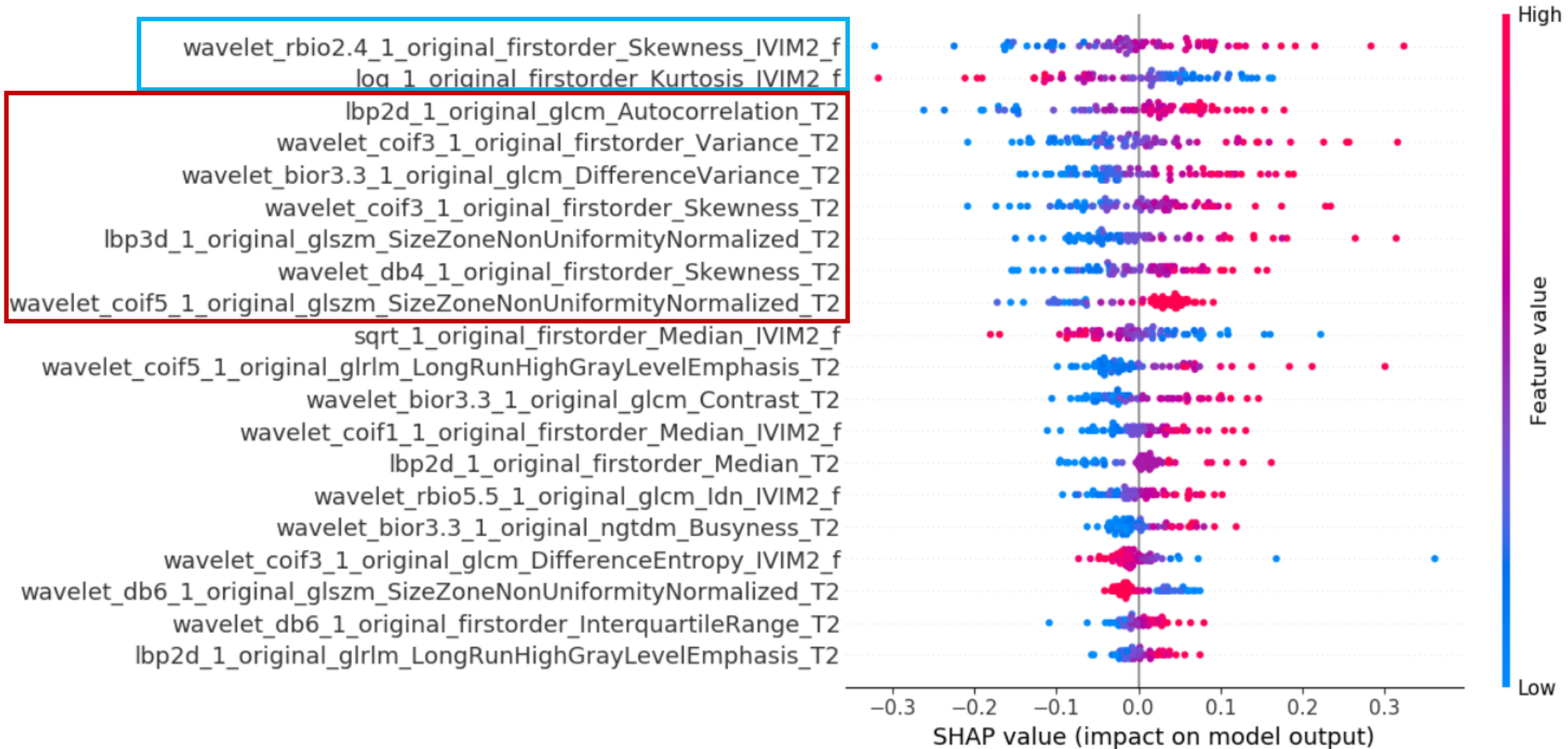
- 202 Pca patients
 - 144 (GS<7)
 - 58 (GS ≥ 7)
- 3210 Radiomic Features
 - First/higher order statistics
 - GLRLM, GLCM, GLSZM, GLDM
 - shape-based 2D and 3D features
 - Logarithmic, Exponential, wavelet transforms
- 4-fold stratified cross validation
- Classifiers
 - LogisticRegression, KNeighborsClassifier,
 - RandomForestClassifier, AdaBoost Classifier,
 - GaussianNB
- Performance Evaluation
 - Sensitivity
 - Specificity
 - Accuracy (ACC)
 - AUC
- Explainability (SHAP)



- The **perfusion-related parameter f** showed better performance compared to other diffusion biomarkers when combined with T2 imaging.
- Very good diagnostic accuracy:
 - **ACC: 80%**
 - **AUC: 85%**

G. S. Ioannidis *et al.*, "Explainable AI Radiomics in Prostate Cancer Aggressiveness Prediction using different quantitative Diffusion MRI models," *2025 47th Annual International Conference of the IEEE Engineering in Medicine and Biology Society (EMBC)*, Copenhagen, Denmark, 2025, pp. 1-7, doi: 10.1109/EMBC58623.2025.11254453.

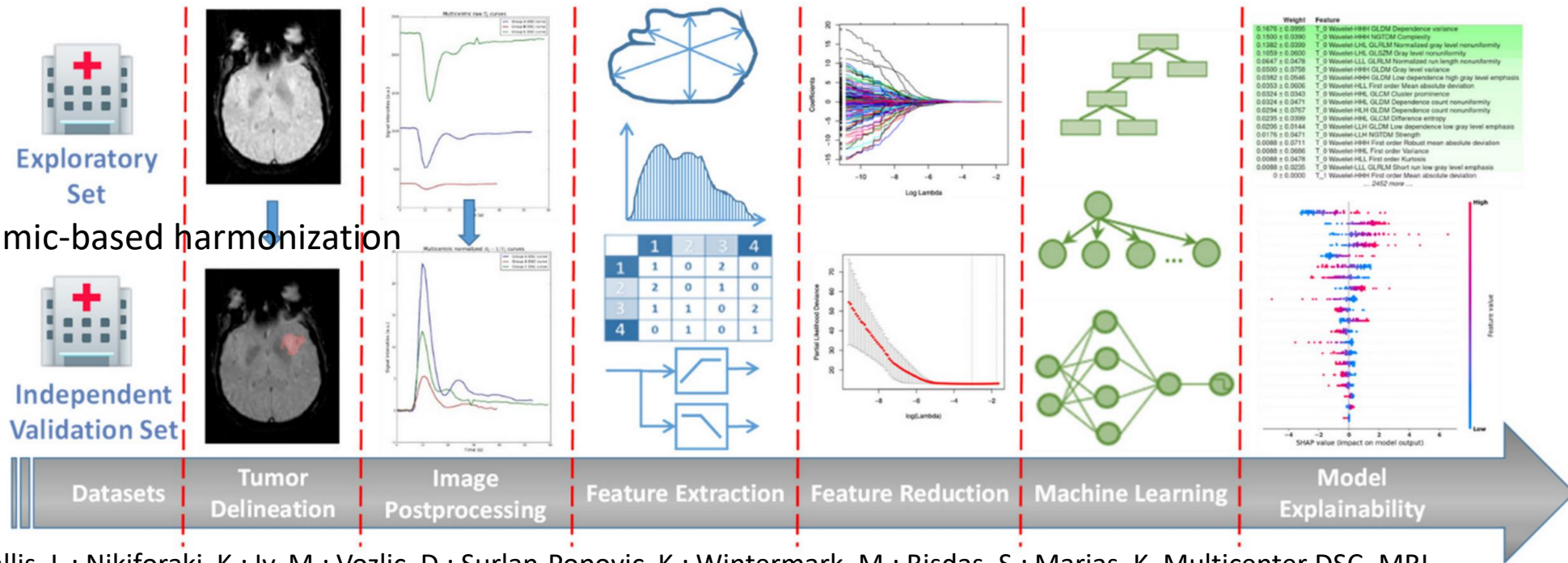
Shap Explainability



Multicenter DSC–MRI-Based Radiomics Predict IDH Mutation in Gliomas

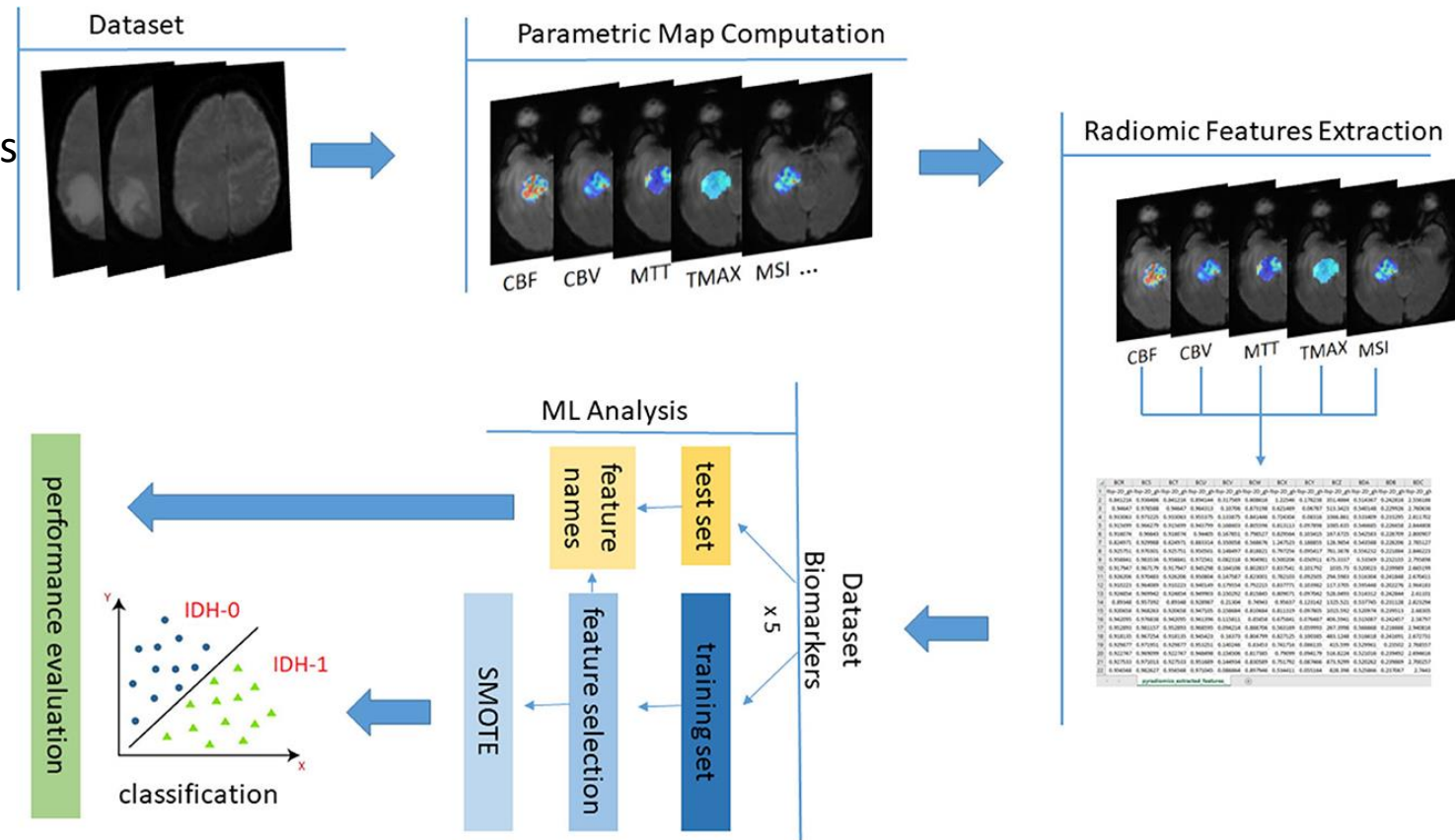
- Radiomics based ML to predict isocitrate dehydrogenase (IDH) mutations in gliomas
- 160 patients underwent dynamic susceptibility contrast magnetic resonance imaging (DSC–MRI)
 - (IDH-mutant = 41, IDH-wildtype = 119)
 - 833 Radiomic features

- Initial performance
 - ACC: 0.544
 - AUC: 0.639
- Performance after Dynamic-based harmonization
 - ACC: 0.706
 - AUC: 0.736

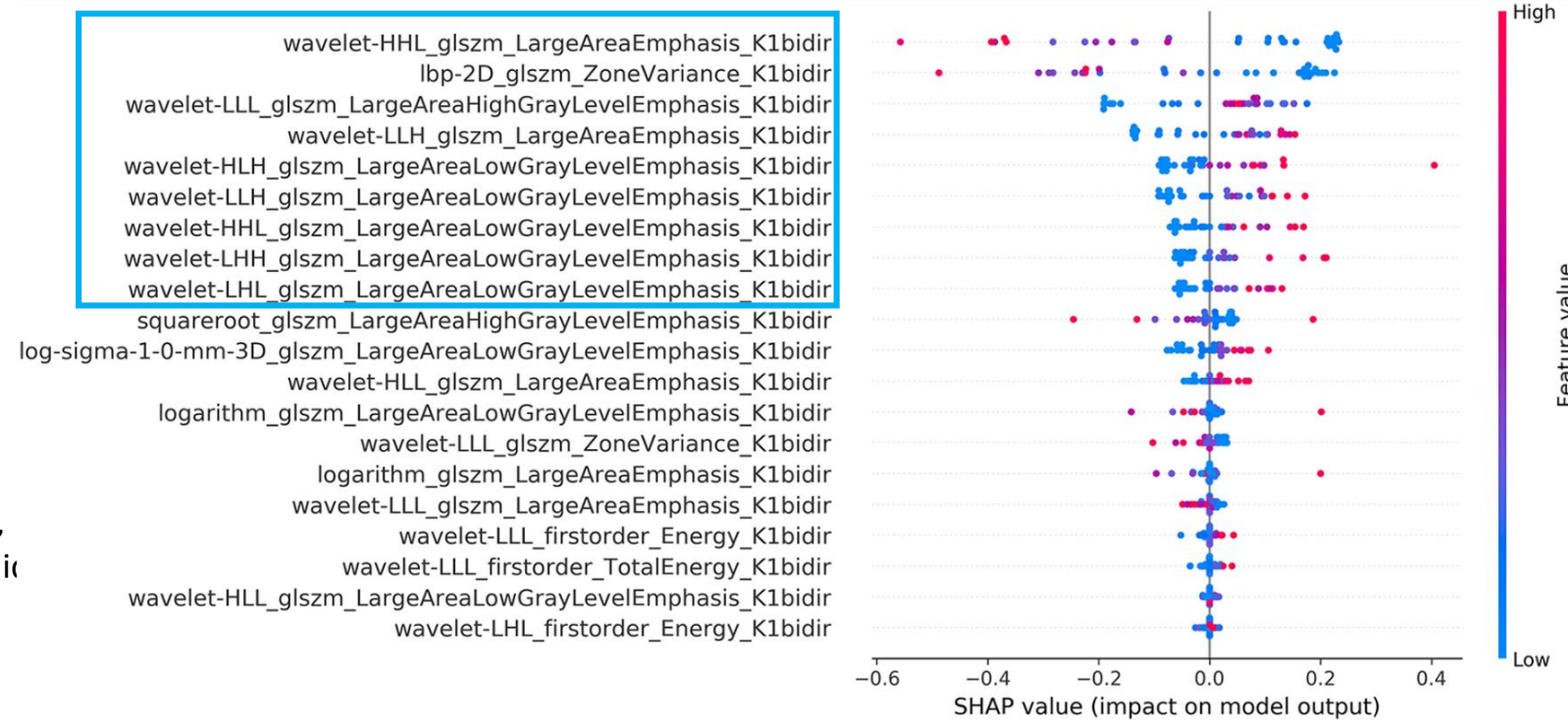
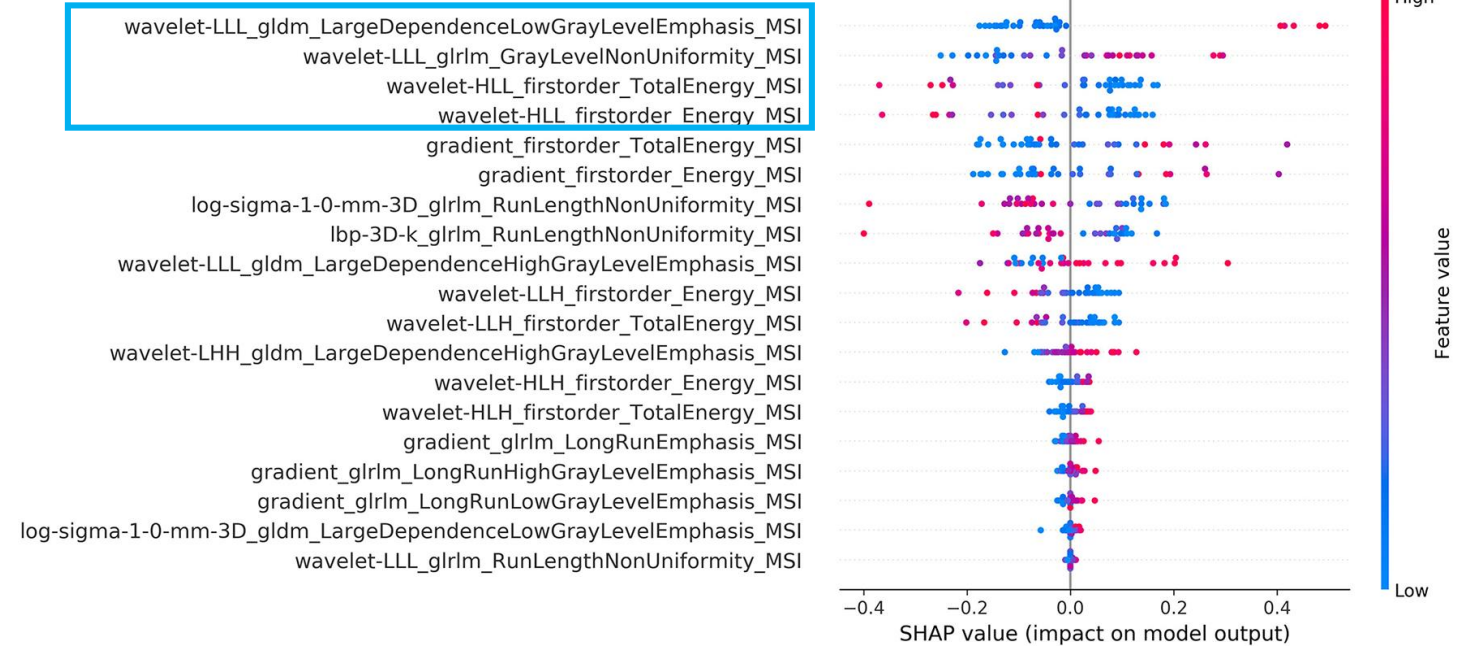


Extending the previous work: Investigating the value of radiomics stemming from DSC quantitative biomarkers in IDH mutation prediction in gliomas

- Biomarker based radiomics to predict isocitrate dehydrogenase (IDH) mutations in gliomas
- 160 patients, Quantitative modeling
 - Gamma fitting, leakage correction algorithms
 - Parametric mapping
 - (rCBF, rCBV, rMTT, MSI, TMAX, K_1 ...)
 - 1734 Radiomic features
- Best performing Parametric maps
 - MSI: (ACC 74.3% AUC 74.2%)
 - K_1 : (ACC 75% AUC 70.5%)

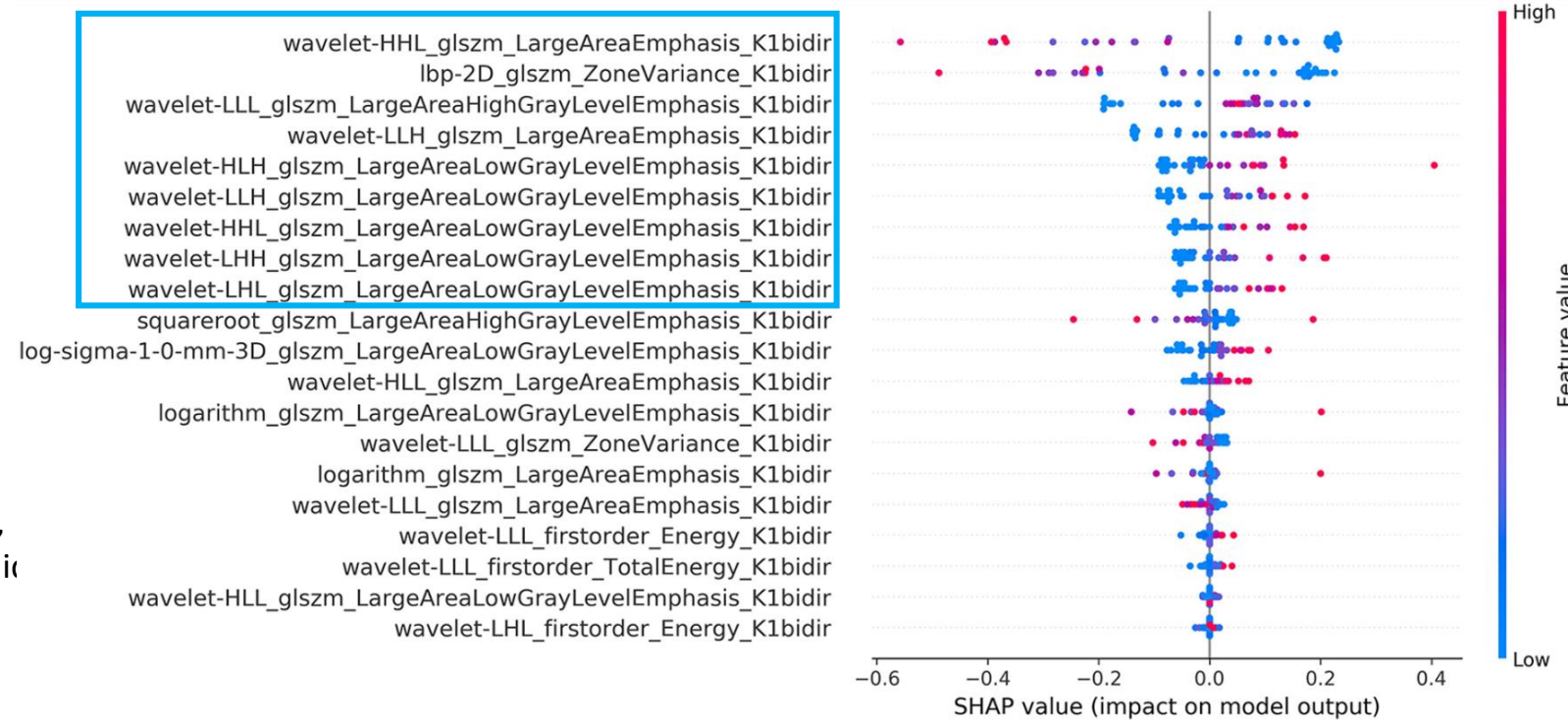
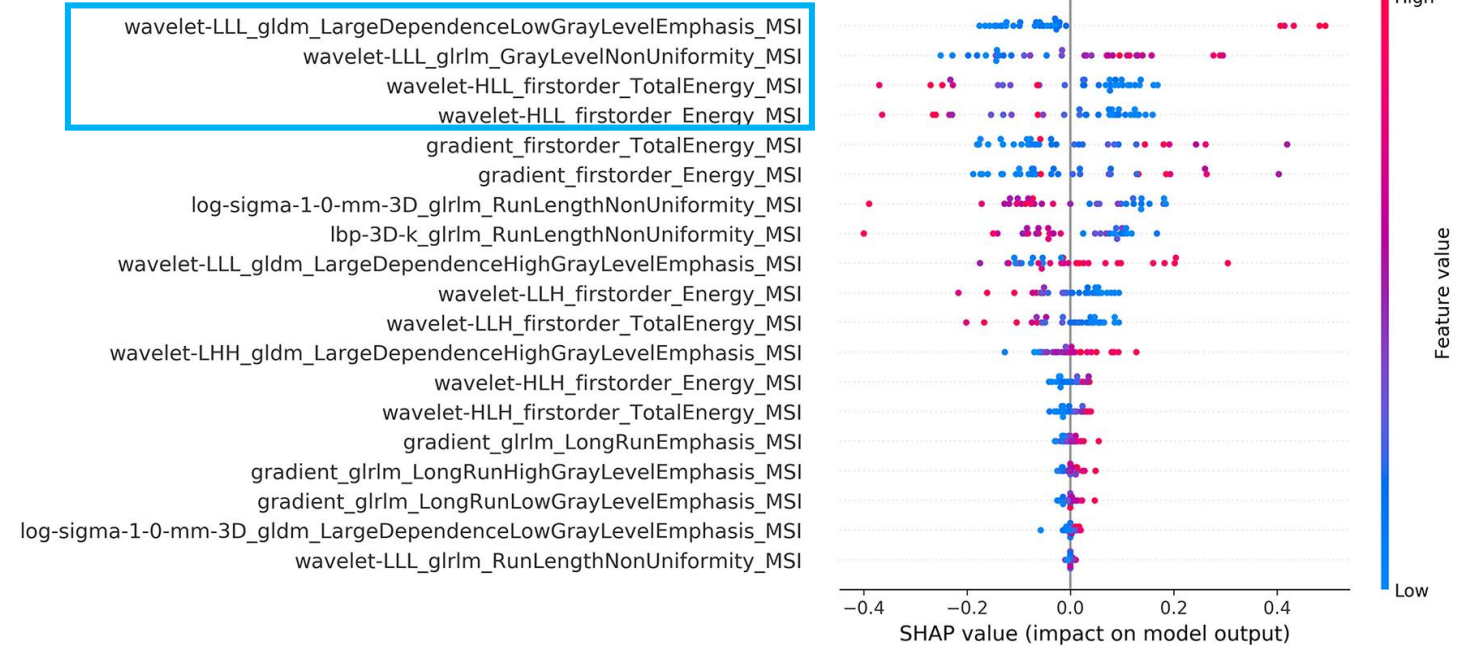


Shap Explainability



Ioannidis GS, Pigott LE, Iv M, Surlan-Popovic K, Wintermark M, Bisdas S and Marias K (2023) Investigating the value of radiomic stemming from DSC quantitative biomarkers in IDH mutation prediction in gliomas. *Front. Neurol.* 14:1249452. doi: 10.3389/fneur.2023.1249452

Shap Explainability

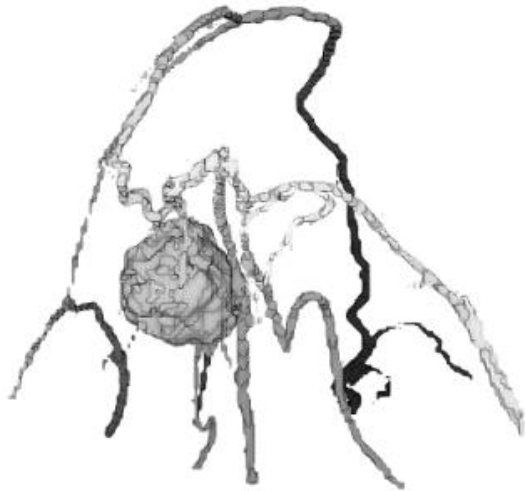


Ioannidis GS, Pigott LE, Iv M, Surlan-Popovic K, Wintermark M, Bisdas S and Marias K (2023) Investigating the value of radiomic stemming from DSC quantitative biomarkers in IDH mutation prediction in gliomas. *Front. Neurol.* 14:1249452. doi: 10.3389/fneur.2023.1249452

Pathologic Complete Response (pCR) prediction

The role of vascular network features and radiomics

- Quantitative Vasculature feature extraction



Quantitative tumor-associated vasculature (QuanTAV) features tool

Novel Radiomic Measurements of Tumor-Associated Vasculature Morphology on Clinical Imaging as a Biomarker of Treatment Response in Multiple Cancers 🛒

Nathaniel Braman ; Prateek Prasanna; Kaustav Bera ; Mehdi Alilou ; Mohammadhadi Khorrami; Patrick Leo; Maryam Etesami; Manasa Vulchi; Paulette Turk ; Amit Gupta ; Prantesh Jain ; Pingfu Fu ; Nathan Pennell ; Vamsidhar Velcheti ; Jame Abraham ; Donna Plecha; Anant Madabhushi  

Morphology features

Features	Description
Statistics of vessel orientation along the XY projection image (f1-f5)	Mean, median (med), standard deviation (std), skewness (skew), and kurtosis (kurt) of local vessel orientations computed across XY vessel map
Statistics of vessel orientation along the XZ projection image (f6-f10)	Mean, med, std, skew, kurt of local vessel orientations computed across XZ vessel map
Statistics of vessel orientation along the YZ projection image (f11-f15)	Mean, std, max, skew, kurt of local vessel orientations computed across XZ vessel map
Statistics of vessel orientation along the rotation-elevation projection image (f16-f20)	Mean, std, max, skew, kurt of local vessel orientations computed across vessel map of rotation and elevation with respect to the tumor
Statistics of vessel orientation along the distance-rotation projection image (21-f25)	Mean, std, max, skew, kurt of local vessel orientations computed across vessel map of distance and rotation with respect to the tumor
Statistics of vessel orientation along the distance-elevation projection image (f26-f30)	Mean, std, max, skew, kurt of local vessel orientations computed across vessel map of distance and elevation with respect to the tumor

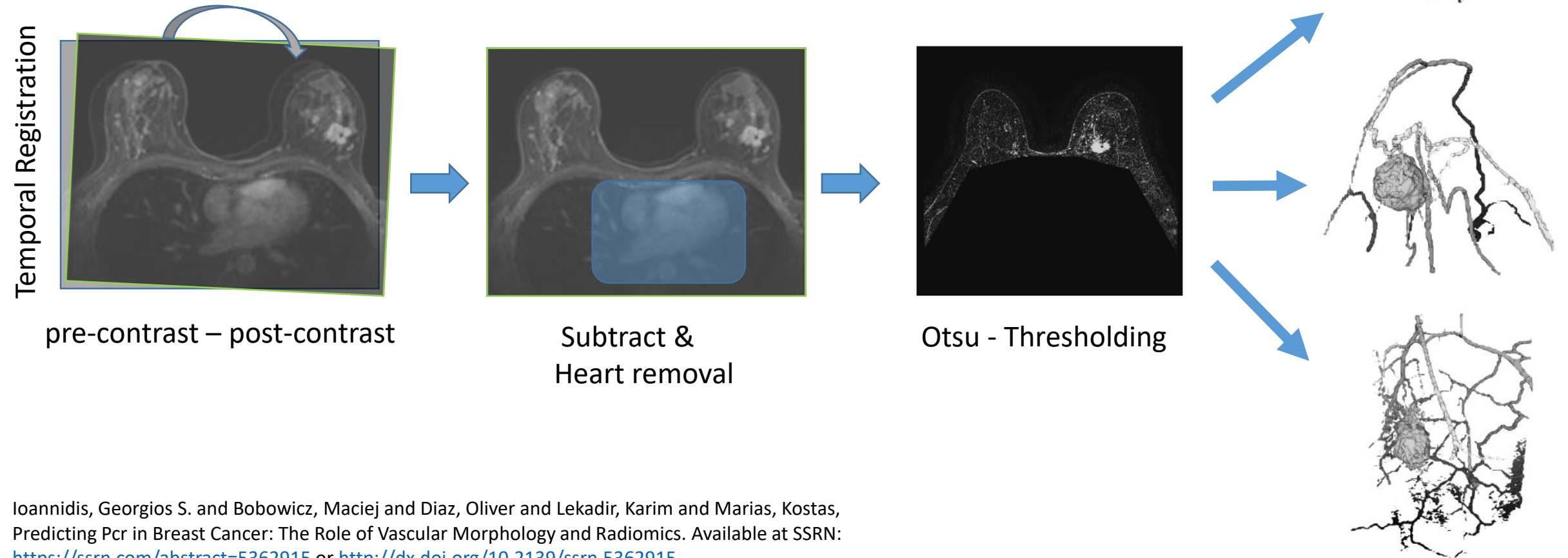
Spatial organization features

Features	Description
Statistics of torsion per branch (f1-f5)	Mean, standard deviation (std), maximum (max), skewness (skew), and kurtosis (kurt) of torsion across all branches
Statistics of curvature standard deviation per branch (f6-f10)	Mean, std, max, skew, kurt of the standard deviation of curvature measured along each branch
Statistics of mean curvature per branch (f11-f15)	Mean, std, max, skew, kurt of the average curvature measured along each branch
Statistics of maximum curvature per branch (f16-f20)	Mean, std, max, skew, kurt of the maximum curvature measured along each branch
Statistics of curvature skewness per branch (f21-f25)	Mean, std, max, skew, kurt of the skewness of curvature measured along each branch
Statistics of curvature kurtosis per branch (f26-f30)	Mean, std, max, skew, kurt of the kurtosis of curvature measured along each branch
Statistics of global vascular curvature (f31-f35)	Mean, std, max, skew, kurt of the curvature measured across all branches combined
Histogram of global vascular curvature (f36-f45)	10-bin histogram of the curvature measured across all points of the vessel volume
Histogram of torsion (f46-f55)	10-bin histogram of the torsion measured across all branches combined
Total vessel volume (f56-f58)	Vessel volume (f56), vessel volume normalized to the total size of the 3D region of interest (f57), vessel volume normalized to the volume of the tumor (f58).
Total vessel length (f59)	Total length of vessels within the region of interest
Tumor feeding branches (f60, f61)	Number (f60) and percentage (f61) of vessel branches that enter the tumor volume from the surrounding tumor environment.

Pathologic Complete Response (pCR) prediction

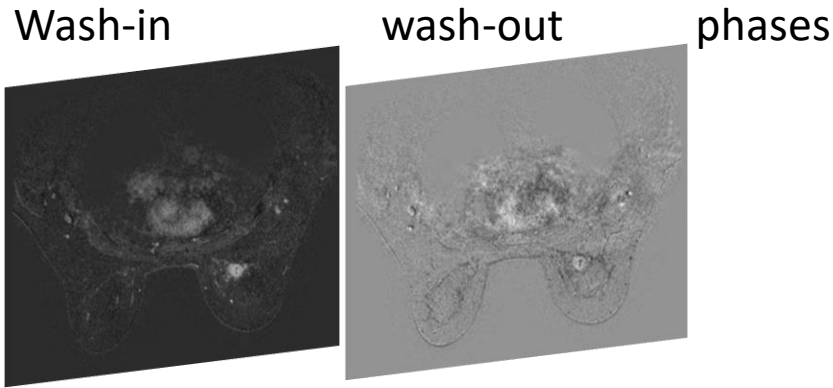
The role of vascular network features and radiomics

- Image pre-processing



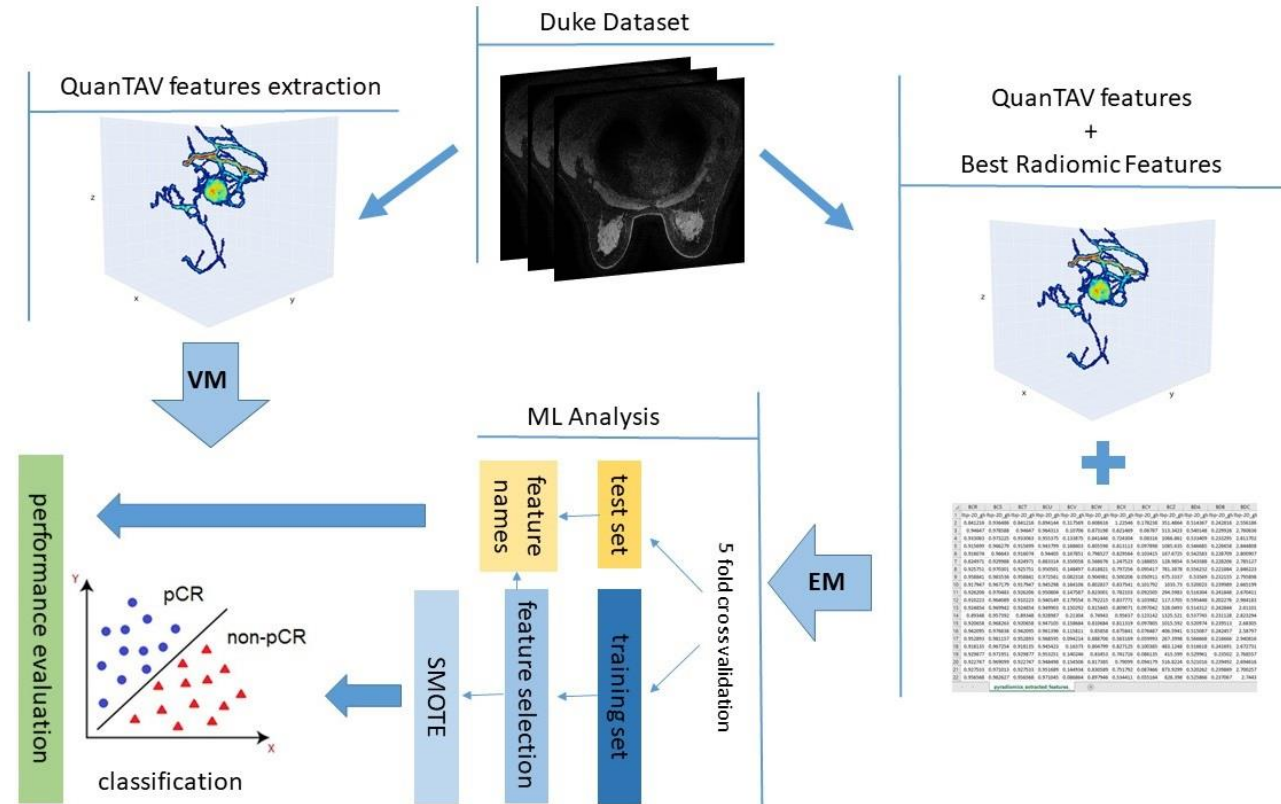
The role of vascular network features and radiomics

Radiomic Features Extraction



Redundancy analysis

	BCR	BCS	BCT	BCU	BCV	BCW	BCX	BCY	BCZ	BDA	BDB	BDC
1	lbp-2D_gli											
2	0.841216	0.936486	0.841216	0.894144	0.317569	0.608616	1.22546	0.178238	351.4864	0.514367	0.242816	2.556186
3	0.94647	0.578588	0.94647	0.964313	0.10706	0.873196	0.621469	0.06787	513.3423	0.540148	0.229926	2.760636
4	0.933063	0.973225	0.933063	0.953375	0.133875	0.841446	0.724304	0.08316	1066.861	0.533409	0.233295	2.811702
5	0.915699	0.966279	0.915699	0.943799	0.168603	0.805596	0.811113	0.097898	1085.635	0.546465	0.226558	2.844808
6	0.916074	0.96643	0.916074	0.94405	0.167851	0.798527	0.829564	0.103415	167.6725	0.542583	0.228709	2.800907
7	0.824971	0.929988	0.824971	0.883314	0.350058	0.568676	1.247523	0.188855	128.9854	0.543588	0.228206	2.785127
8	0.925751	0.970301	0.925751	0.950501	0.148497	0.818821	0.797256	0.095417	781.3878	0.556232	0.221884	2.846223
9	0.958841	0.983536	0.958841	0.972561	0.082318	0.904981	0.500206	0.050911	675.3337	0.535669	0.232155	2.795898
10	0.917947	0.967179	0.917947	0.945298	0.164106	0.802837	0.837541	0.101792	1035.73	0.520023	0.239989	2.665199
11	0.926206	0.970483	0.926206	0.950804	0.147587	0.823001	0.782103	0.092505	294.5983	0.516304	0.241848	2.670411
12	0.910223	0.964089	0.910223	0.940149	0.179554	0.792215	0.837771	0.103982	117.3705	0.595448	0.202276	2.964183
13	0.924854	0.969942	0.924854	0.949903	0.150292	0.815845	0.809071	0.097042	528.0493	0.514312	0.242844	2.61101
14	0.89348	0.957392	0.89348	0.928987	0.21304	0.74943	0.95637	0.123142	1325.521	0.537745	0.231128	2.823294
15	0.920658	0.968263	0.920658	0.947105	0.158684	0.811084	0.811319	0.097805	1015.592	0.520974	0.239513	2.68305
16	0.942095	0.978638	0.942095	0.961396	0.115811	0.85858	0.675841	0.076487	406.5941	0.515087	0.242457	2.58797
17	0.952893	0.981157	0.952893	0.968595	0.094214	0.888706	0.561169	0.059993	267.3998	0.566668	0.216666	2.940916
18	0.918135	0.967254	0.918135	0.945423	0.16373	0.808799	0.827125	0.100385	483.1248	0.516618	0.241891	2.672731
19	0.929877	0.971951	0.929877	0.953251	0.140246	0.83453	0.741716	0.086135	415.599	0.529961	0.23502	2.768557
20	0.922747	0.969099	0.922747	0.948498	0.154506	0.817385	0.79099	0.094179	516.8224	0.521016	0.239492	2.694616
21	0.927533	0.971013	0.927533	0.951689	0.144934	0.830589	0.751792	0.087466	873.9299	0.520262	0.239869	2.700257
22	0.956568	0.982627	0.956568	0.971045	0.086864	0.897946	0.534411	0.055164	828.398	0.525866	0.237067	2.7443

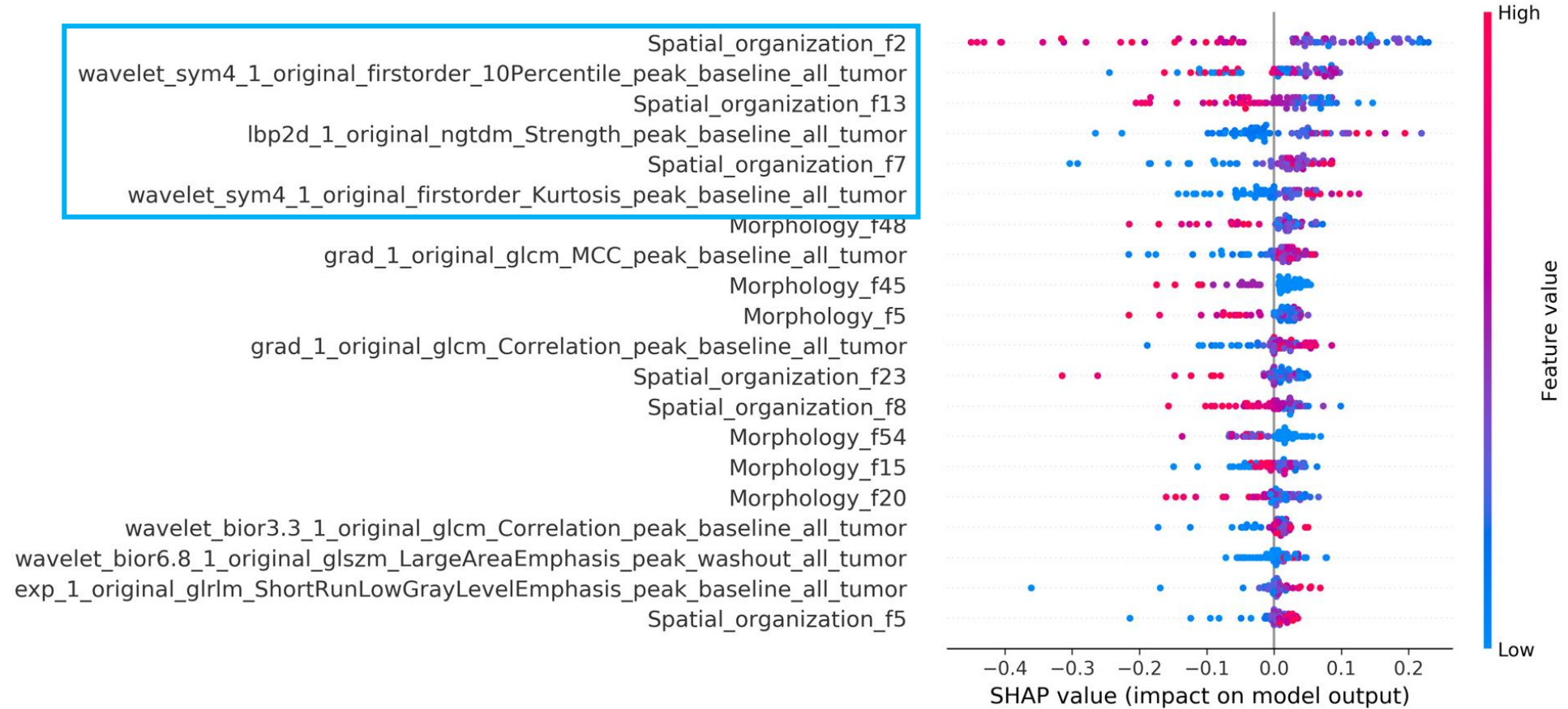


Radiomics Prediction of Pathologic Complete Response to Neoadjuvant Chemotherapy in Breast Cancer: Interpretation and Imaging Pitfalls

Georgios S. Ioannidis, Smriti Joshi, Grigorios Kalliatakis, Katerina Nikiforaki, Vassilis Kilintzis, Haridimos Kondylakis, Oliver Diaz, Maciej Bobowicz, Karim Lekadir & Kostas Marias

Wash-in : subtraction of the first dynamic phase from the baseline
 Wash-out : subtraction of the first pass from the last dynamic phase

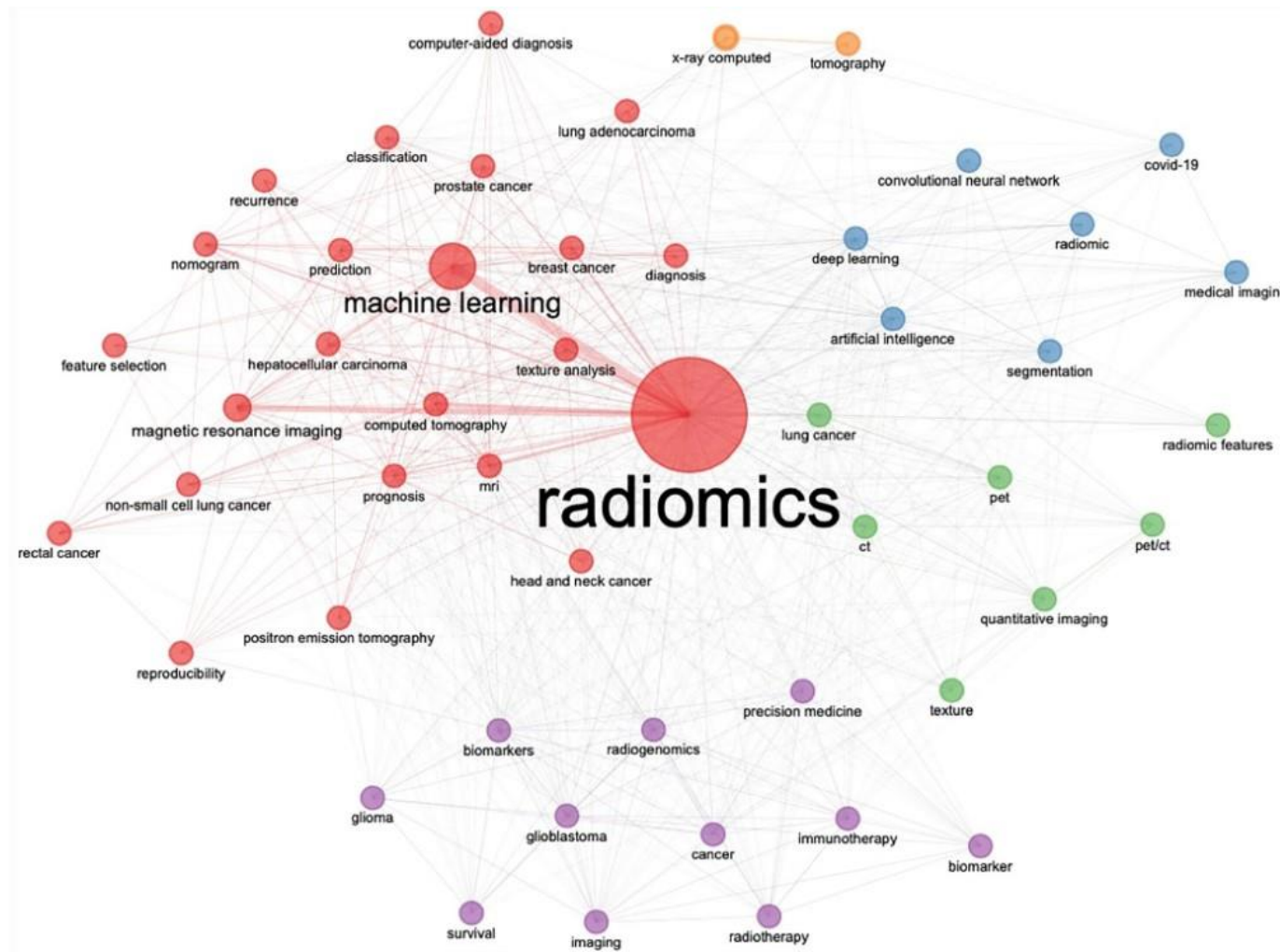
Shap Explainability



Conclusion

- Cancer Imaging with MRI
- Quantitative MRI
- Radiomics
- Build an AL model for eHealth applications
- Explainability
 - Further investigation in wavelet decomposition of an image
 - Biomarkers found to explain why the classifier took the decision
 - Synergy of Clinical Experts and AI people towards more : **Robust**
Generalizable AI models

Thank you for your attention!



PCa RADical PATH



Any questions?